Czech Technical University in Prague
Faculty of Electrical Engineering
Department of Control Engineering

Dynamic system identification methods for fMRI data processing

DOCTORAL THESIS

January 2013 Ing. Jana Nováková

Czech Technical University in Prague
Faculty of Electrical Engineering
Department of Control Engineering

Dynamic system identification methods for fMRI data processing

by

Ing. Jana Nováková

Supervisor: Ing. Martin Hromčík, Ph.D.

Dissertation submitted to the Faculty of Electrical Engineering of
Czech Technical University in Prague
in partial fulfillment of the requirements for the degree of

Doctor

in the branch of study
Control Engineering and Robotics
of study program Electrical Engineering and Informatics

January 2013

To my family.

Preface

The system identification methods for fMRI data processing are presented in this research work. fMRI is very important diagnostic method especially in neurology, neurosurgery and psychology. The key issue is to apply some system identification methods for fMRI data processing and consider future practical application as a certain alternative to commonly used statistical methods.

I started my work on biomedical topic as a graduate student within my Diploma thesis under Dr. Zdeněk Hurák supervision, (FEE, CTU in Prague), and in co-operation with the Department of Neurology, 1^{st} Faculty of Medicine, Charles University in Prague. Then I continued as Ph.D. student on research topic with supervisor Dr. Martin Hromčík, (FEE, CTU in Prague). We together joined some research projects of Department of Neurology - Writer's cramp study and Essential tremor study and to provide fMRI data and posturography data processing.

First and foremost, I would like to express my gratitude to my supervisor Dr. Martin Hromčík giving me an opportunity to join his research team, for creating perfect conditions for my research, for encouragement and motivation and for introducing me to the world of research.

Thanks to fruitful discussions and mutual interactions with members of the Department of Neurology - professor Evžen Růžička, Dr. Robert Jech and Dr. Martina Hoskovcová. I also wish to thank my colleagues at the Department of Control Engineering at Czech Technical University in Prague, especially to Dr. Zdeněk Hurák, Dr. Tomáš Haniš, Dr. Petr Kujan, Jan Rathouský, Pavel Hospodář, for creating enjoyable and inspiring environment. My deepest obligation comes to my parents for bringing me up and supporting during studies. I would like to give some words of thanks to my beloved husband Ondřej and my small daughter Věra for their support and sympathy.

Concerning the financial arrangements, this work was supported by the Ministry of

Education of the Czech Republic under Research Program No. MSM6840770038 and by Centre of Applied Cybernetics 1M0567.

Jana Nováková

Czech Technical University in Prague
Prague, January 2013

Dynamic system identification methods for fMRI data processing

Ing. Jana Nováková

Czech Technical University in Prague, Prague, January 2013

Supervisor: Ing. Martin Hromčík, Ph.D.

The thesis deals with application of system identification methods for fMRI data processing. The main goal of this thesis is to define the complex dynamic system represented by brain areas within the context of the systems theory, and to cast it as a task for system identification procedures. The system, as interpreted by the systems theory, is a complex object consisting of interconnected subsystems and components which transforms inputs into outputs and this transformation can be characterized by a mathematical model, usually in the form of differential equations. The key issue is to look for these models by identification methods and to consider them as a certain alternatives for fMRI data processing to commonly used statistical methods.

We focus especially to DCM procedure for detection of the brain intrinsic structure and we review that from user's point of view within Writer's cramp study. Then we propose application of modern multidimensional systems identification algorithms of the subspace identification theory in the context of fMRI data analysis. The methods originated in 1990s in the field of process control and identification and yield robust linear model parameter estimates for systems with many inputs, outputs and states. Our ultimate goal was to establish an alternative to the DCM analysis procedure which would eliminate its main drawbacks, namely the need to pre-define the models structure.

Contents

List of Figures

List of Tables

Chapter 1

Introduction

1.1 Motivation

The main goal of the dissertation thesis is to formulate advanced concepts and procedures/algorithms commonly used in process identification for fMRI research field and to apply the system identification methods for fMRI data modeling. Human brain can be described as a system consisted of many subsystems representing constituent brain areas which represents a dynamical system with characteristic dynamics. By means of fMRI technique it is even possible to measure output signals of this complex system so we know the input-output behavior of the system and we suppose it is possible to use identification and estimation methods to describe that by linear system with a certain accuracy. This approach could provide an important information about some crucial parameters of the brain system and it could be a certain alternative to available statistical techniques which are commonly used for fMRI data processing at present. The thesis reports on some attempts to approach the problem of modeling of simple system including just one brain area and looking for dynamics description of more complex system with several brain areas. It also brings a comprehensive survey of related literature, mainly out of the systems and control field.

The thesis was partly created in cooperation with Department of Neurology, 1^{st} Faculty of Medicine, Charles University in Prague (professor Evžen Růžička,

Dr. Robert Jech).

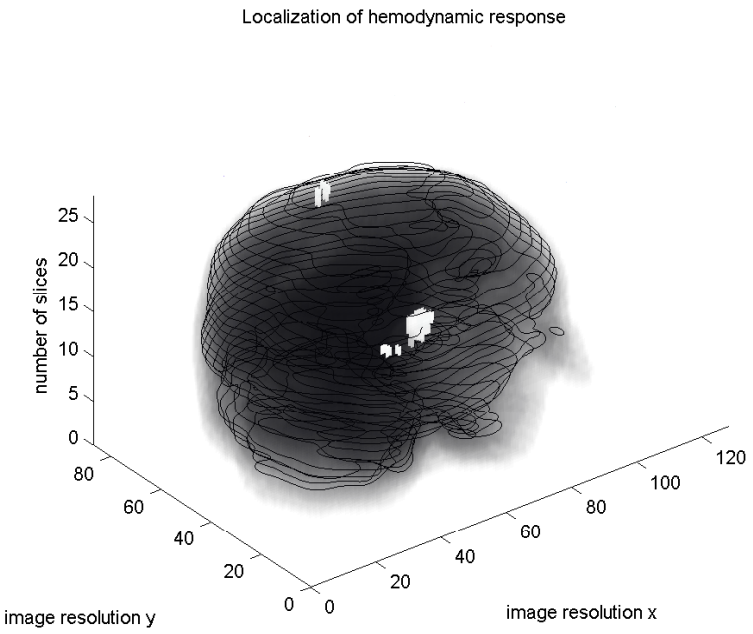

Figure 1.1: Illustrative picture

1.2 Outline of thesis

The following second chapter gives the specific goals and objectives of the dissertation thesis. All of them are then discussed in further chapters.

The third and fourth chapters contain the basic information about fMRI technique and data processing by commonly used tool for Matlab called SPM toolbox and they bring some details necessary to comprehension of the other chapters.

Next fifth chapter deals with the clinical study - Writer's cramp study - completed in cooperation with Department of Neurology, 1^{st} Faculty of Medicine, Charles University in Prague. Our personal experience with SPM toolbox for DCM procedure is discussed with real fMRI data giving some details, advantages and drawbacks.

The sixth chapter deals with fMRI data modeling by system identification

methods. It discusses the results of the modeling depending on fMRI data quality. It also considers the subspace identification methods as an alternative to DCM procedure for intrinsic structure detection.

In the seventh chapter, the results of the thesis are summed up and confronted with the goals and objectives set. There are also summarized the scientific achievements of this thesis and outlines immediate opportunities for improvement and further research.

Chapter 8 contains the publications of the authors, related directly to the thesis, and other references used throughout the text.

1.3 State of the Art

A detailed overview and survey literature related to commonly used techniques for fMRI data processing is in the first part of State-of-the-art. The next part brings overview of modeling and estimation techniques used for process identification which could be potentially useful as an alternative for fMRI data processing.

1.3.1 fMRI data processing field

fMRI is a special type of MRI technique for brain activity mapping. The basic BOLD principle, monitoring changes in oxygenation of blood by BOLD signal (Blood Oxygen Level Dependence), is known since 1990. The first successful study with fMRI technique using was published by Jack W. Belliveau and col. in 1991 (Belliveau, J. W. and col., 1991).

In 1994 Karl Friston decided to develop a software for biomedical data processing on basis of statistical analysis and he created the first version of Statistical Parametric Mapping (SPM) toolbox with help from John Ashburner, Jon Heather, Andrew Holmes and Jean-Baptiste Poline. It was defined especially for data from Positron Emission Tomography (PET). Next improved versions, based on the SPM'94, were extended for fMRI data, EEG data etc. The fundamental principles and algorithms implemented in SPM toolbox for fMRI data processing are summarized by Friston et al.(Friston, K. J. et al., 2007), briefly overview was published by Smith (Smith, S. M., 2004). Bayesian estimation techniques

also used in SPM toolbox are described in (Friston, K. J. et al., 2002) and (Friston, K. J., 2002). The fundamental papers concerning fMRI data modeling are also published by Friston and his colleagues and they are given in next section. Here we also refer to some techniques for brain intrinsic structure detection. The crucial point concerning this topic is work of Karl Friston (Friston, K. J. et al., 2003) about Dynamic Casual Modeling (DCM).

1.3.2 Biophysical models

This category includes Balloon and Hemodynamic model which describe effect of external input to result BOLD signal by input-state-output model with four state variables, see below for details. Unknown parameters (means and variances of their distributions) of these models are then estimated from measured data by means of Bayesian scheme with iterative expectation maximization algorithm, see (Friston, K. J., 2002) for details. This procedure is used in DCM as well.

1.3.2.1 Balloon and Hemodynamic model

Balloon model, demonstrated in (Buxton, R. B. and Frank, L. R., 1997) and (Buxton, R. B. et al., 1998), is a nonlinear dynamical model with two state variables - blood volume v and deohyhemoglobin content q. It is an input-state-output model, described by Equations 1.1 considering blood flow f_{in} as an input signal and BOLD signal y as an output (BOLD signal - ratio between oxyhemoglobin and deoxyhemoglobin content). Increasing blood flow causes venous balloon inflating and deohyhemoglobin is expelled faster. It means increasing BOLD signal. There can be also clear small dip in BOLD signal caused by lack of oxyhemoglobin at the beginning of the process. Then the blood flow peaks, however it relaxes slower than deohyhemoglobin content, so we can observe small poststimulus undershoot in BOLD signal. Balloon phenomenon can be described by following differential state equations and output equation.

$$
\begin{aligned}
\dot{v_i} &= \frac{1}{\tau_i}\left(f_{in} - v_i^{\frac{1}{\alpha}}\right) \\
\dot{q_i} &= \frac{1}{\tau_i}\left(f_{in}\frac{E(f_{in},E_0)}{E_0} - v_i^{\frac{1}{\alpha}}\frac{q_i}{v_i}\right) \\
y_i &= V_0\left(k_1\left(1-q_i\right) + k_2\left(1-\frac{q_i}{v_i}\right) + k_3\left(1-v_i\right)\right) \\
E(f_{in},E_0) &= 1-\left(1-E_0\right)^{\frac{1}{f_{in}}},
\end{aligned}
\tag{1.1}
$$

where τ_i is time constant called Hemodynamic transit time, α is Grubb's exponent and E_0 is Resting oxygen extraction fraction. These parameters fall into group of biophysical parameters whose mean and variance can be estimated by Bayesian methods. So the Balloon model deals with the link between blood flow and BOLD signal. However there exists Hemodynamic model which adds two extra state variables and represents relationship between synaptic activity and BOLD response.

The Hemodynamic model, see Equations 1.2 essentially combines the Balloon model and linear model of cerebral blood flow iniciated by neuronal activity. It includes two state variables s - vasodilatory signal and f_{in} - blood flow, see differential equations below.

$$
\begin{aligned}
\dot{f_{in}} &= s \\
\dot{s} &= \epsilon u(t) - \frac{s}{\tau_s} - \frac{f_{in}-1}{\tau_f}
\end{aligned}
\tag{1.2}
$$

$u(t)$ is neuronal activity and ϵ, τ_s and τ_f are the unknown biophysical parameters determining dynamics of hemodynamic model. The estimation of these biophysical parameters is completed in (Buxton, R. B. et al., 1998), (Friston, K. J. et al., 2000), (Friston, K. J., 2002) and (Friston, K. J. et al., 2003) and it is also important part of DCM procedure. Simulink model including Hemodynamic and Balloon part is depicted in Figure 1.2. Very interesting paper from estimation and filtering point of view concerning biophysical parameters estimation was published by Zhenghui Hu (Zhenghui, H. et al., 2009) in 2009. He used unscented Kalman filter for nonlinear analysis of the BOLD signal.

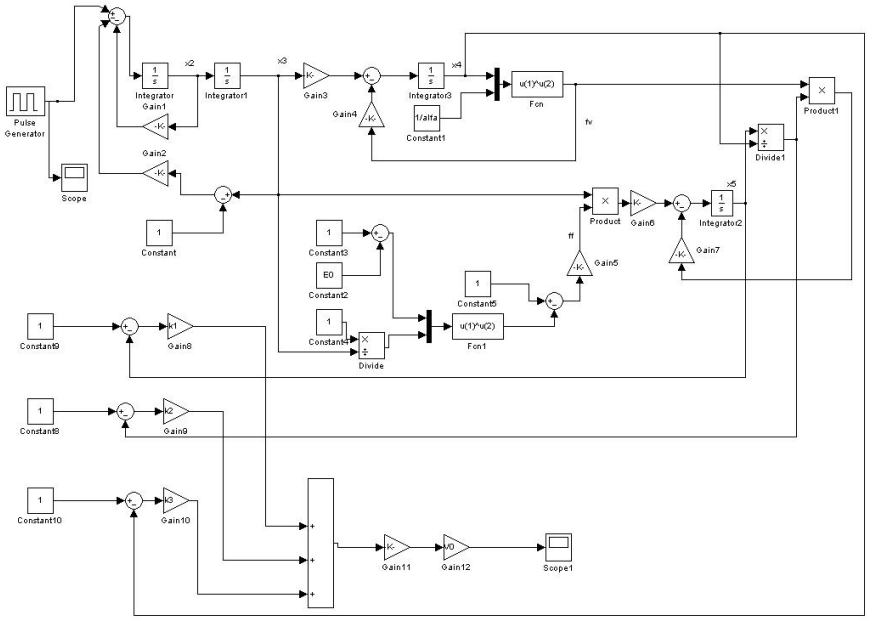

Figure 1.2: The nonlinear model of brain dymanics

1.3.3 Convolution models

The standard convolution model consider each voxel as linear time-invariant system. Convolution of stimulus function with so-called HRF (Hemodynamic Response Function) gives the predicted response which is part of GLM (General Linear Model). These models are used in SPM toolbox in the 1^{st} level analysis, see chapter 4. Nice review about convolution models is in (Friston, K. J. et al., 1994).

1.3.4 Brain structure detection

Some techniques, mainly statistical, are dedicated for brain structure detection. They are often a follow-up to basic fMRI modeling procedures. Here we provide just short overview.

Nowadays, inference about connectivity or coupling among brain areas, using fMRI, usually rests upon some form of Dynamic Causal Modeling (DCM). DCM

uses Bayesian techniques to identify the underlying neuronal system in terms of coupling parameters. Crucially, one has to specify prior constraints on the sparsity or form of the connections and then test different models (forms) of connectivity. DCM is used to compare mathematical models with and without specific connections which entails fitting or inverting different models and then comparing their evidence. It is a methodology which enumerates possible models first, and then tests their validity using the conventional tools for testing statistic hypotheses (Friston, K. J. et al., 2003). The details are mentioned in chapter 4.
In addition to DCM there exist other methods modeling effective connectivity among brain areas. MAR (Multivariate autoregressive) models describe the regional BOLD signal as a linear combination of past data vectors whose contributions are weighted by the parameter matrices, see (Harrison, L. M. et al., 2003). The next methods are Granger causality mapping (Roebroeck, A. et al., 2005), PPI (psychophysiological interactions) models (Friston, K. J. et al., 1997) and ICA (Independent Component Analysis) (Calhoun, V. D. et al., 2003).

1.3.5 System identification methods

In this thesis we deals with using system identification methods for fMRI data processing and we apply especially parametric identification methods. Very nice overview of system identification methods and basic identification principles is given in (Ljung, L., 1999). Some practical aspects of identification are described in (Verhaegen, M. and Verdult, V., 2007). We decided to use subspace identification methods for modeling of fMRI data from more brain areas (MIMO system identification) especially for their numerical stability and good quality results for MIMO system identification. The first important starting point for our research concerning subspace identification methods was book of Peter van Overschee and Bart de Moor (Overschee, P. V. and Moor, B. D., 1996) from University of Leuven who provided the important basic details and explained some principles of subspace identification. The other crucial works concerning application of subspace identification methods were (Katayama, T., 2005), (Garnier, H. and Liuping, W., 2008), (Favoreel, W. et al., 2000). Similarity transformation of linear systems used for transformation of identified model to more suitable form

is described in detail (Antsaklis, P. J. and Michel, A. N., 1997).

Chapter 2

Goals and objectives

Specific goals of this dissertation were set as follows:

1. Develop a comprehensive review of techniques and procedures used in the fMRI area from the systems and process identification viewpoint. Focus on the process of fMRI measurement, discuss the fMRI data structure and present other issues concerning fMRI which could be helpful for the application of systems identification procedures in this area.

2. Get familiar with the "State of the Art" techniques used in fMRI data processing, namely with Dynamic Causal Modeling (DCM). Verify them with experimental data coming from a clinical study. Established partnership with Department of Neurology, 1^{st} Faculty of Medicine, Charles University in Prague is supposed to be exploited. Discuss the results and identify advantages and drawbacks of the standard fMRI modeling techniques.

3. Develop alternatives to fMRI data processing procedures, namely to Dynamic Causal Modeling, based on process identification and estimation techniques. Demonstrate them with simulated and experimental fMRI data.

Chapter 3

fMRI overview

This chapter brings the overview of fundamental principles and characteristics of fMRI which is a special type of MRI technique. It serves as a necessary background for fMRI data processing and for better insight to next chapters.

3.1 Introduction

fMRI is one of several functional mapping methods (in addition to EEG - Electroencephalography, MEG - Magnetoencephalography and PET - Positron Emission Tomography technique, see (Bailey, D. L. et al., 2005), (Hämäläinen, M. et al., 1993) and (Cohen, D. and Halgren, E., 2004) for details) which notice physiological changes related to brain activity. fMRI is able to detect brain area activity resulting from cognitive, motoric or another stimulation and it can give high quality visualization of brain functions. It therefore uses particularly in neurophysiological research, within some neurosurgical intervention and also in psychology (Smith, S. M., 2004). There are two fundamental principles of fMRI measure - perfusion fMRI and more often used BOLD fMRI, first demonstrated by Seiji Ogawa (Ogawa, S. et al., 1990). The perfusion fMRI provides an absolute measure of blood flow whereas the second method BOLD fMRI (Blood Oxygen Level Dependent) uses the ratio between oxygen and deoxygen blood. fMRI measurement is then set of BOLD signals representing brain activity in some brain

areas. A dimension of mapped brain area is defined by technical equipment. It is however possible to declare that fMRI features excellent spatial resolution (down to 1x1x1mm) but quite weak time resolution (in the order of seconds) which is sufficient for functional brain mapping in neurophysiological research, unfortunately it can be restricting for some techniques used in process identification.

3.2 MRI principle

MRI principles and specifications are described in (Geuns, R. J. et al., 1999), (Hornak, J. P., 2008). Here we provide just short report of MRI principle.
The basic MRI principle is based on changes of magnetic property of hydrogen atoms (especially protons and their spin characteristics) with significant magnetic moment. In external magnetic field magnetic moments of atoms are in one of two possible positions - parallel (low energy state) or anti-parallel (high energy state) with the direction of external magnetic field. In addition to this aligning all protons precess with some frequency called Larmor which is determined by strength of magnetic field and gyromagnetic ratio (specified for each type of nucleus). The result magnetization M_0 (consider many protons in observed tissue)

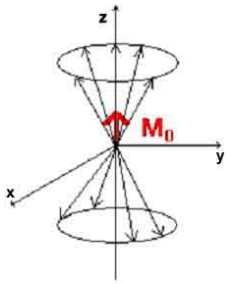

Figure 3.1: External magnetic field - adopted from (Masaryk University Brno, 2012)

is oriented with external magnetic field (in z-axis direction) which means it is not possible to measure that see Figure 3.1. So it is necessary to tip result magnetization into XY plane where receiver coil can induced voltage corresponding result magnetization. It can be reached by using RF pulses with the same frequency as Larmor frequency which cause that individual spins begin to precess in phase.

Some spins in lower energy state also absorb energy (it is possible thanks to equality of the Larmor frequency and frequency of RF pulses) and resonance of spins comes up. Due to this phenomenon the technique is called magnetic resonance. It induces changing value of magnetization vector in z-axis direction, see Figure 3.2. Then result magnetization vector performs rotation in XY plane with Larmor frequency and coil induces voltage as in Figure 3.3. With RF pulse finishing the process called relaxation starts - it means nuclei spins return to original position and magnetization vector tips back to Z plane. It is possible to define two time relaxation constants T_1 and T_2. T_1 is time when result magnetization Mz reaches 63% of original amplitude. T_2 is defined as the time when M_{xy} falls to 37% of its maximum value, see (Masaryk University Brno, 2012) for details.

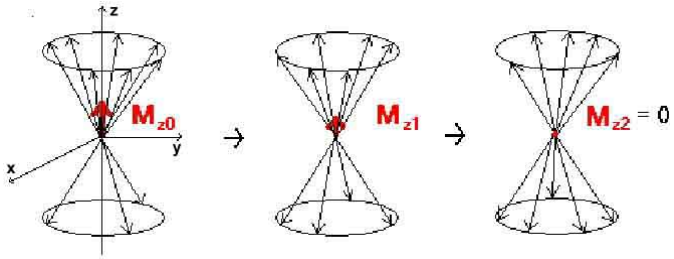

Figure 3.2: The change of result magnetization due to RF pulse absorption - adopted from (Masaryk University Brno, 2012)

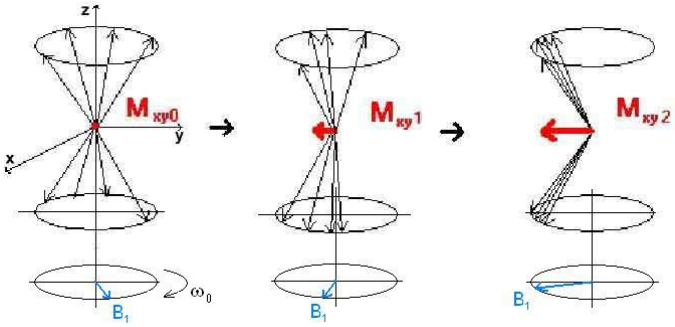

Figure 3.3: Tipping of result magnetization vector due to RF pulse absorption - adopted from (Masaryk University Brno, 2012)

3.3 BOLD signal

fMRI is a special type of MRI measurement with external stimulation, for example fingers motion, pictures projection, electrical stimulation etc. The most used principle of fMRI measurement is BOLD which uses the fact that the oxygen is transported by hemoglobin and therefore the ratio between oxygen and deoxygen blood changing with on-off stimulation signal in active areas is measured. It is based on different magnetic features of oxyhemoglobin (diamagnetic) with little effect to magnetic field and deoxyhemoglobin (paramagnetic) which causes inhomogeneity in nearby magnetic field (Miyapuram, K. P., 2008).
So measured BOLD signals bring information about physiological changes in some brain areas and we can observe so-called hemodynamic responses in BOLD signals measured in active areas. In an simplified way it is possible to describe the basic phenomenon thus, see Figure 3.4. With brain (neural) activity, utilization of oxygen is rapidly increased in active brain area (brain tissue) and it causes initial very small negative undershoot (oxygen consumption is so large so ratio oxygen/deoxygen decreases). Then blood flow is increased in active area which causes increasing of oxyhemoglobin, inhomogeneities in magnetic fields and more intensive BOLD signal. After neural activity (external input or stimuli) finishing, blood flow and oxygen/deoxygen ratio decrease to original value. But the change of blood flow is slower so we can also observe negative undershoot at the end of signal.

3.4 fMRI measurement and data structure

This section brings some information related to some specific features and terminology concerning fMRI BOLD measure and fMRI data structure.
Time repetition is interval between measured images. We can also call it as sampling period. For each fMRI measurement it is necessary to design appropriate input/stimuli signal, so-called fMRI experiment. The crucial point is anyway to ensure different BOLD value (level) for active and passive part because of detection of hemodynamic response in set of measured BOLD signals. So for successful

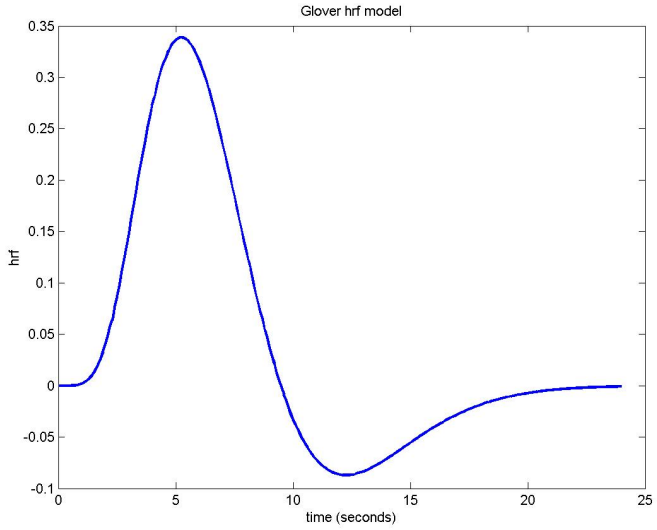

Figure 3.4: Characteristic shape of a hemodynamic response - adopted from (of Mathematics and Statistics, 2012)

fMRI measurement the experiment design is very important part. Here is a certain analogy with process identification where sufficient input/exciting signal guarantees a good starting point for successful identification process. So there exist two basic types of fMRI experiments:

- Epoch/Block design - Stimulation events are put into blocks which is beneficial to obtain high intensity of BOLD signal for active segment. It is useful for statistical analysis but it is not possible to detect accurate shape of hemodynamic response, see Figure 3.5.

- Event design - It is able to ascertain the correct shape of hemodynamic response by short stimulation events with sufficient distance for damping of previous response, see Figure 3.6.

We can also classify the experiment design according to physiological brain function. It is possible to study senzomotoric functions, emotion, memory, speech action, visual and perception or cognitive functions.

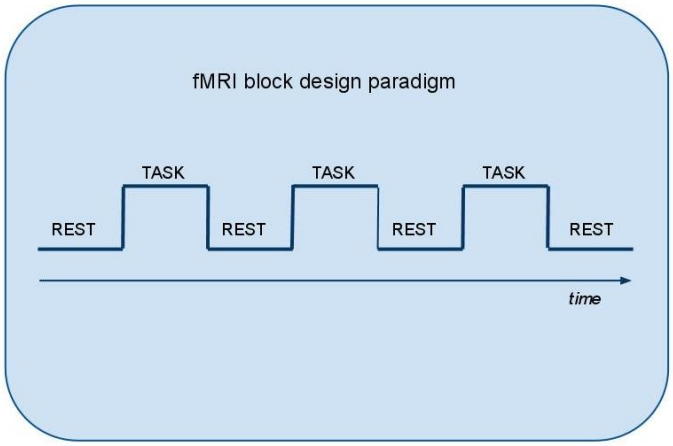

Figure 3.5: Block design - adopted from (Radiopaedia.org, 2012)

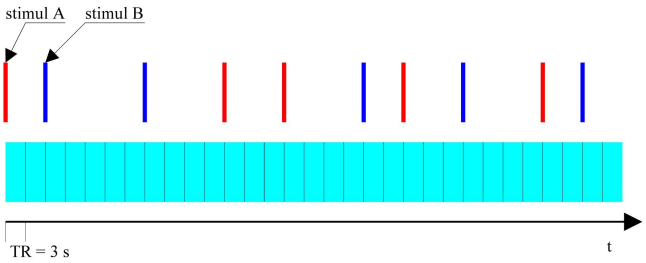

Figure 3.6: Event-related design - adopted from (Masaryk University Brno, 2012)

The result of fMRI measurement is fMRI data with special structure. fMRI data set is sequence of images, so-called scans, corresponding with time axis. Each scan maps brain activity in one time point and it is divided into several slices which are usually characterized by good spatial resolution. Each slice is comprised from voxels representing small brain area/tissue. All terms concerning fMRI data structure are clarified in the Figure 3.7. In fact we consider each scan (image) as a 3D matrix representing BOLD values measured in many brain areas and set

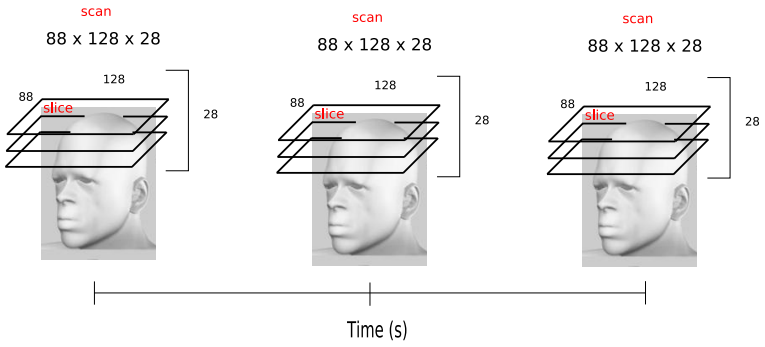

Figure 3.7: fMRI data structure

of such matrices measured in different time points forms BOLD time series for brain areas. Consequently the result of one fMRI experiment is time sequence of three-dimensional matrices representing time progress of brain activity (it means changes of BOLD signals in time) in particular brain areas. We can say that from process identification point of view the problem of spatial localization and modeling of a response to a specific stimulation (visual, acoustic, electrical) is cast as an analysis of the response of a 3D array (cube) of dynamic systems with the goal to localize those SISO systems that "resemble" some model best.

3.5 fMRI features

We can state that fMRI is very useful technique of brain function imaging. It has some advantages in comparison with EEG, MEG and PET. EEG and MEG have relatively poor spatial localization and it is also necessary to use high number of electrodes. PET technique is invasive imaging method and it presents radiation load. To the contrary fMRI is noninvasive, with high spatial and satisfactory temporal resolution and number of hospitals with adequate fMRI equipment is increased. However we can say that fMRI technique has also some constraints during fMRI data processing primarily. It also poses higher financial claims. Further constraints are insufficient knowledge of functional brain organization which can be very restricting for interpretation of results.

Chapter 4

SPM toolbox

4.1 Introduction

The SPM toolbox is a noncommercial Matlab package implementing statistical tools for neuroimaging data processing (fMRI, PET, EEG, MEG). SPM toolbox is developed at the Department of Imaging Neuroscience, University College London (SPM toolbox, 2012) in research group of Karl Friston, see Figure 4.1 with logotypes of all toolbox versions. The main principle of SPM tool is creation of continuous statistical processes to test hypotheses about regionally specific effects (Friston, K. J. et al., 1991). The most often used statistical analysis of fMRI data is called voxel-by-voxel analysis because it is based on testing signal of each scanned voxel (elementary capacity of scanned brain, see previous chapter for details about data structure). This analysis usually compares measured BOLD signal with experimental paradigm which is defined by fMRI experiment, see previous chapter - section 3.4, and predefined characteristic shape of hemodynamic response. The result of the testing is a statistical map with marking of active brain areas (represented by voxel or cluster of voxels).

One of the crucial applications of the SPM toolbox is the first level analysis consisting in the detection of active brain areas for one patient. The second level analysis, also covered by the SPM toolbox, is related to processing of fMRI data across the whole patients group. Besides these functions, the toolbox offers tools

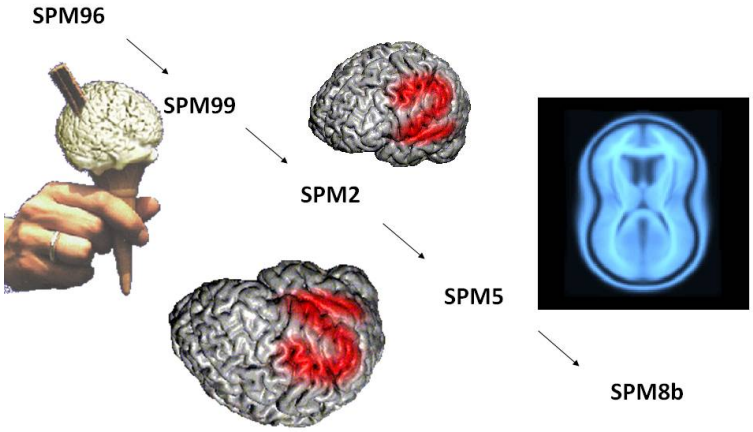

Figure 4.1: SPM toolbox logotypes - adopted from (SPM toolbox, 2012)

for DCM analysis (intrinsic structure detection), such as the parameters estimation routines, tools for comparison of resulting models, and a function for averaging models across the whole patients group. In addition there are also implemented some preprocessing procedures preparing correct data for next processing, see Figure 4.2 with GUI of SPM8 characterizing all basic functions of the toolbox.

4.2 fMRI data processing steps

4.2.1 Preprocessing steps

The first level of fMRI data analysis is usually data preprocessing - preparation of data for statistical analysis, especially reduction of artifacts and noise and normalization for future comparison. Below described routines of temporal and spatial processing are implemented in SPM toolbox. However, it is not necessary to use all of them, it depends on following data processing, see (SPM toolbox manual, 2012) and (Masaryk University Brno, 2012) for details.

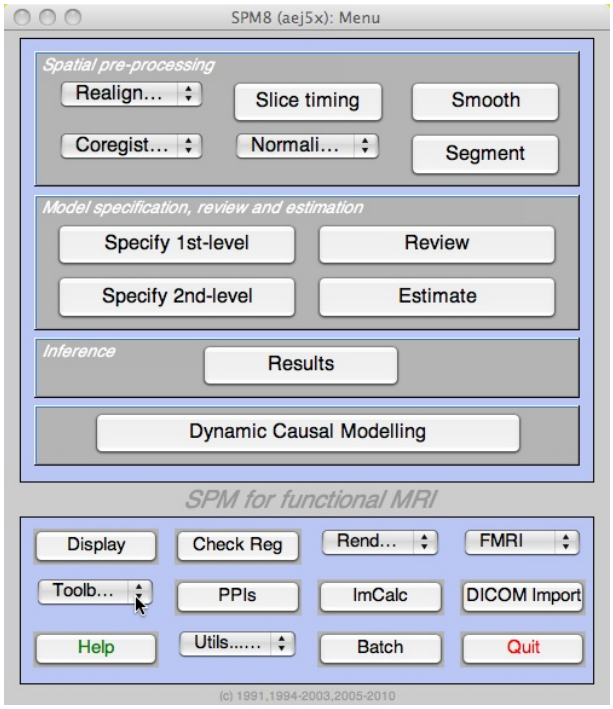

Figure 4.2: GUI of SPM8 toolbox - adopted from (SPM toolbox, 2012)

4.2.1.1 Temporal processing

- Slice timing - Each scan is usually acquired as a sequence of some slices which however are not taken in the same time point. This routine shifts the data (each voxel's time series) as if whole scan was acquired at exactly the same time. It is accomplished by a simple shift of the phase of the sines that make up signal (SPM toolbox manual, 2012).

4.2.1.2 Spatial processing

- Realign - Each measurement is affected by patient's undesirable artifacts - spontaneous head motion (heartbeat, respiration). Realigning corrects movement artifacts in time-series of images using least squares algorithm and spatial transformation (translation and rotation), see Figure 4.3. One scan is appointed as a reference to which the rest of scans are realigned.

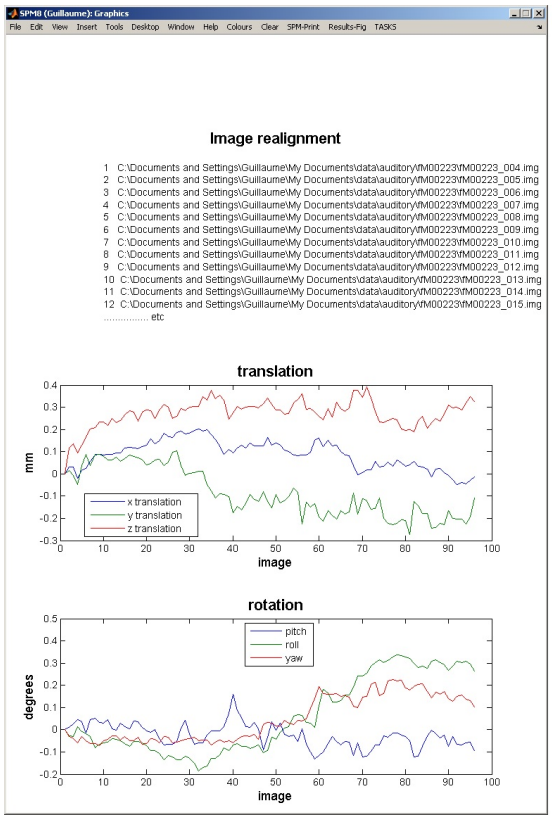

Figure 4.3: Realign procedure - created in SPM toolbox

- Normalize - Sometimes it is useful to compare results of some subjects mutually or to average images (signals) across subjects. This procedure transforms all scans into standardized space defined by template images (for instance commonly used Talairach standard space) and it uses the affine transformation and nonlinear deformation for that.

- Smooth - This routine is implemented for noise suppression by filtration of high spatial frequencies using Gaussian kernel with specified width.

- BOLD intensity normalization - It normalizes BOLD time-series intensity which can vary during individual acquisitions and it could cause incorrect detection of active voxels.

The preprocessing steps are very important for later statistical analysis and they usually increase the statistical validity. However it is necessary to think over which steps and parameters are suitable to apply.

4.2.2 First level analysis

After preprocessing steps the fMRI data is ready for statistical analysis. Brain activity is mapped by so-called Statistical Parametric Mapping with detection of voxels activated by stimulation. This procedure is called the first level analysis and it is usually voxel-by-voxel principle. The methods of this one-dimensional analysis include linear regression, t-tests, correlation, ANOVA technique etc. Almost all of them require some model of assumed BOLD signal which can be created as convolution of fMRI experimental design and predefined hemodynamic response shape. All these statistical procedures are based on GLM - General Linear Model - specifying conditions by design matrix corresponding with experimental design. GLM expresses BOLD signal as a linear combination of explanatory variables X and error term ϵ, see Equation 4.1, in fact it is linear regression - special case of GLM. This can be considered in matrix form as

$$Y = \boldsymbol{X}\boldsymbol{\beta} + \boldsymbol{\epsilon}, \tag{4.1}$$

where $\mathbf{X}$ is design matrix and β parameter to estimated. It can be solved by least squares algorithm, see Equation 4.2.

$$\beta = (\boldsymbol{X}^T\boldsymbol{X})^{-1}\boldsymbol{X}^T\boldsymbol{Y} \tag{4.2}$$

The design matrix is constructed by convolution of temporal experimental design and basis function defined by canonical hemodynamic response function (HRF). The final result is a statistical map with localization of brain neural activity resulting from appropriate statistical inferences testing (t-statistic, z-statistic). The Figure 4.4 presents one result of the first level analysis. In this case the stimulation was left hand motion. The activated voxels are colorfully marked. Details of the first level analysis are mentioned in (Boynton, G. et al., 1996) (Friston, K. J., Ashburner, J., Frith, C. D., Poline, J. B., Heather, J. D. and Frackowiak, R. S. J., 1995) (Friston, K. J., Holmes, A. P., Wors-

LEY, K. J., POLINE, J. B., FRITH, C. D. and FRACKOWIAK, R. S. J., 1995).

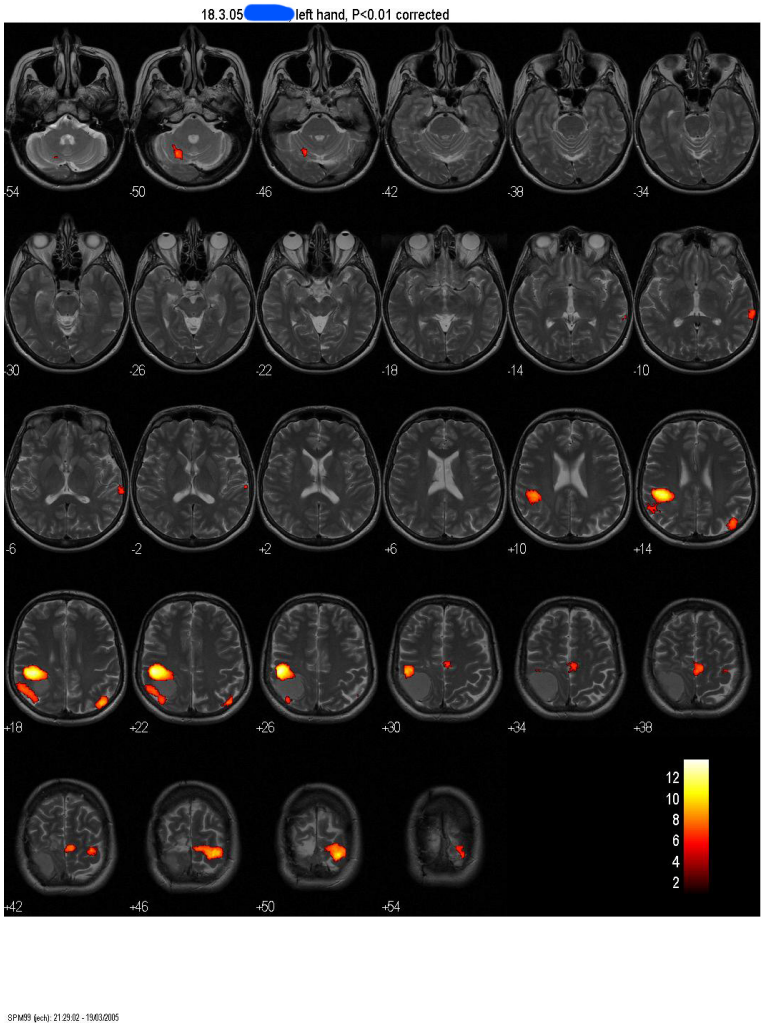

Figure 4.4: The first level analysis result - active areas are marked - adopted from Dr. Robert Jech, Department of Neurology, 1^{st} Faculty of Medicine, Charles University in Prague

4.2.3 Second level analysis

By the second level analysis we can generalize our findings beyond subjects we have studied. There exist statistical methods for combining results across the subjects. The result is statistical map as well and it is valid for all patients from investigated group. These methods include "fixed-effects" and "random-effects" procedures (Holmes, A. and Friston, K., 1998). Fixed-effects allow inferences to be made about the particular subject in the experiment, while random-effects allows inferences to be made about the population. Random effects analysis is considered more appropriate for fMRI research because it deals with making inferences on the population.

4.3 DCM analysis

DCM (Dynamic Causal Modeling) is a statistical technique for detection of interconnections among selected brain areas (Friston, K. J. et al., 2003), (Kiebel, S. J. et al., 2006), (Penny, W. D. et al., 2004), (Ethofer, T. et al., 2005). DCM assumes a bilinear model in the form Equation 4.3 and the interconnections among brain areas are qualitatively and quantitatively characterized by its parameters (note the presence of so-called modulatory inputs that modulate interconnections directly).

$$\begin{aligned} \dot{x}(t) &= (\boldsymbol{A} + \sum_{j=1}^{M} u_j(t)\boldsymbol{B}_m^j)x(t) + \boldsymbol{B}u(t) \\ y(t) &= \boldsymbol{C}x(t) + \boldsymbol{D}u(t), \end{aligned} \tag{4.3}$$

where $\boldsymbol{A}$ is effective connectivity matrix for interconnections among areas, $\boldsymbol{B_j}$ is effective connectivity matrix encoding the changes in intrinsic connections induced by j^{th} modulatory input u_j, and matrix $\boldsymbol{B}$ representing strength of extrinsic inputs leading directly to brain areas, see Figure 4.5. DCM procedure then combines the bilinear neuronal model Equation 4.3 of interacting areas with the biophysical model by Friston, based on principles of the Hemodynamic model and Balloon

model, detailed mentioned in State-of-the-art, which describes how the unmeasured neuronal activity in a given brain area is transformed into the hemodynamic responses measured by the fMRI. The input signal is generally a deterministic on-off function representing stimulation process (stimuli such as finger movement commands, projection of emotional pictures).

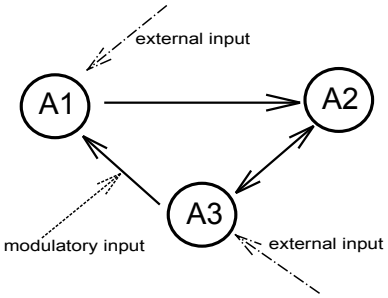

Figure 4.5: Brain areas A1, A2, A3, intrinsic connections among them and two types of input signals - a representative of a predefined model

The first two steps of DCM analysis are selection of several brain areas, described by coordinates of voxel (volumetric pixel) cluster, and definition of inferences (hypotheses) about the area interactions which will be confronted with real fMRI data in the statistical hypothesis-testing manner. The hypotheses usually result from clinical experience and empirical knowledge of a neurologist, trained in functional brain organization. The necessity to rely on an expert in this step can be regarded as a drawback of this method and full enumeration of all possible interaction structures is combinatorially prohibitive. The final step - testing statistical hypotheses - can be computationally very demanding, it can easily take up to a few days on a regular PC. DCM procedure advantages and drawbacks from user's point of view will be discussed in chapter concerning writer's cramp study, see chapter 5.

The DCM models are estimated using Bayesian estimators. The inferences about connections are made using the posterior or conditional density (Friston, K. J. et al., 2003). The DCM result is the likeliest model accompanied by strength values of significant connections, see Figure 4.6.

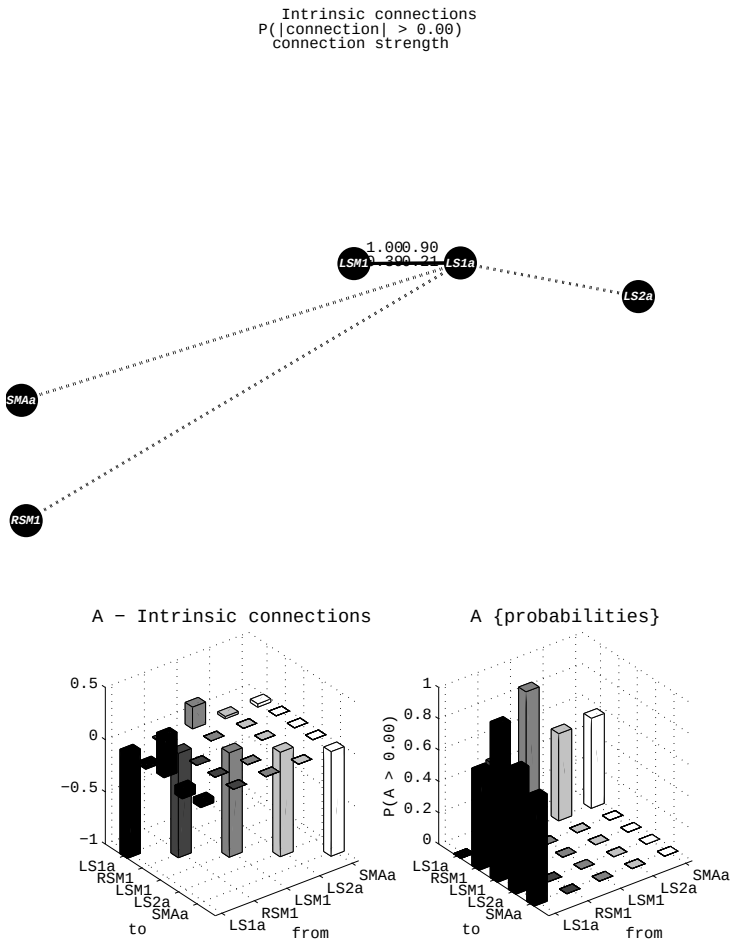

Figure 4.6: Result of DCM procedure - created in SPM toolbox

4.4 SPM toolbox useful tips

4.4.1 Useful functions

I would like to mention two important functions of SPM toolbox which are able to import fMRI data to Matlab workspace. By *spm_vol.m* and *spm_read_vols.m* we can obtain three-dimensional array characterizing one scan of brain - BOLD values measured in same time point.

4.4.2 DCM data simulator

The additional part of SPM toolbox is DCM data simulator which generates the fMRI DCM data according to our requirements. The simulator is started by means of function named *spm_dcm_create*. The function is able to generates BOLD signals of selected brain areas with required parameters such as the signal-to-noise ratio, the number of areas, interscan interval (TR, sampling period in principle), number of scans (samples), number of conditions (stimuli inputs) and the vectors of onsets and durations of input signals (block design features in fact). It is also necessary to define the connectivity matrix A, the input matrix C and the modulatory matrix B, see previous section to bilinear form used for multiple area brain system modeling.
However we have to carefully consider the data generation process because of discrepancies between nonlinear model used in SPM toolbox simulator and nonlinear models published in crucial papers concerning DCM (Stephan, K. E. et al., 2004) (Friston, K. J., 2002) (Friston, K. J. et al., 2000). They differ slightly not only in constants but also in differential equations describing hemodynamic response process.

Chapter 5

Writer's cramp study

This chapter summarizes the Writer's cramp study - project of the Department of Neurology, 1^{st} Faculty of Medicine, Charles University in Prague. We participated in the study by DCM analysis of fMRI data acquired during second phase of the project - Advanced study. The final result of the project was joint paper published in NeuroEndocrinology Letters (Havrankova, P. et al., 2010).

5.1 Introduction

The writer's cramp is a common type of focal dystonia which manifests by involuntary spasm of the hand and forearm muscles (Havrankova, P. et al., 2010). The conventional therapy is the botulotoxin medication, sometimes without clinical effect unfortunately. The next alternative for some patients is an experimental therapy by rTMS - repetitive Transcranial Magnetic Stimulation. rTMS applies the sequence of magnetic pulses by coil focused on defined cortex area causing symptoms suppression. Within the writer's cramp study, we processed fMRI data sets measured before and after rTMS therapy for comparison. We completed DCM analysis as one part of an objective assessment of rTMS therapy effect.

5.2 Materials and methods

12 patients (8 women and 4 men) with right hand writer's cramp were included in the study. The duration of their disorder was 2-11 years. Each patient underwent two five-day blocks of rTMS, the first was real rTMS, the second was sham (placebo) rTMS. The rTMS took 30 minutes every day. The fMRI measurement was carried out before the therapy began (the first day) and after the therapy was finished (the fifth day).

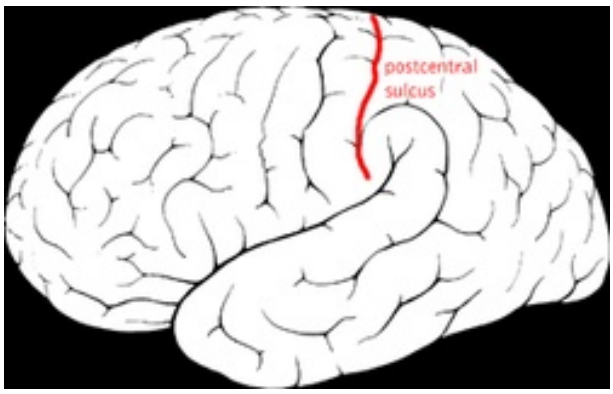

Figure 5.1: Magnetic coil location - adopted from Wikipedia

rTMS was done by 70-mm double coil connected to stimulator. One pulse set contained 1800 pulses. The coil was focused on sulcus postcentralis, see Figure 5.1. fMRI procedure was related to the task with active movement of right hand fingers. The patients were required to perform about ten movements during 6 minutes, each movement with 3 seconds duration. The movements were captured by the video-fMRI monitoring (Jech, R. et al., 2008). As a result, two vectors were obtained for each patients and they contained the onsets (start instants) and durations of movements. The vectors served for fMRI analysis (the detection of statistical significant areas with hemodynamic response) in SPM toolbox ver.5 (SPM toolbox, 2012). All related details on the fMRI procedure and fMRI analysis are described in (Jech, R. et al., 2008).

5.3 DCM

The main task of DCM analysis was to quantitatively approve an effect of the rTMS therapy. All the patients passed clinical examination before and after the therapy. The clinical examination consisted in a subjective assessment by a patient himself, and objective assessments by raters, for instance evaluation of cribbing of text for two minutes see Figure 5.2. The subjective and objective assessments showed significant improvement of writer's cramp symptoms for 9 patients who finished the therapy. For detailed results concerning all assessment, in addition to DCM analysis, see (Havrankova, P. et al., 2010).

The DCM analysis was called to confirm these results. 9 patients finished the rTMS therapy and their fMRI data was put subject to the overall processing. DCM analysis was created only for fMRI data related to real stimulation and measured before and after the therapy. The data was processed separately and then particular connections and their strength were compared. Next to the results themselves, our goal was also to describe experience with the DCM tools of SPM ver.5 for Matlab (SPM toolbox, 2012), based on a specific medical experiment data processing.

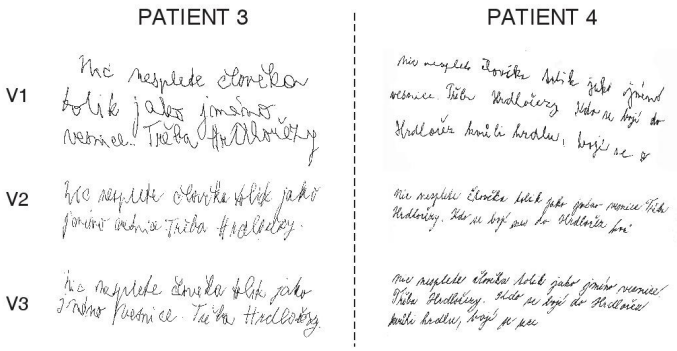

Figure 5.2: The handwriting of patient 3 and patient 4 before rTMS (V1), immediately after the last session of rTMS (V2), and one week later (V3) - adopted from (Havrankova, P. et al., 2010)

5.3.1 Models

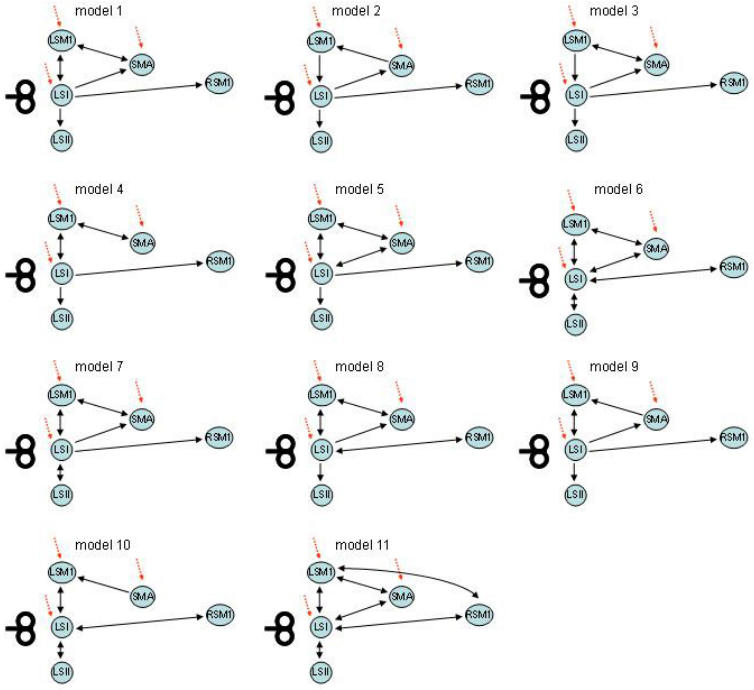

Figure 5.3: Models for DCM procedure

The first step of DCM analysis was the definition of models which were confronted with real data. The definition usually results from clinical experience and from knowledge in functional brain organization. Originally, models which differed in number of connections for data measured before and after the therapy were considered for these reasons. The reasoning behind was a presumption that rTMS could have some influence on functional brain organization and more connections could be detected for data measured after therapy. The problem here was however that the results of DCM analysis for data measured before and data measured after are not easily and directly comparable in this case. Since the DCM approach is based on hypotheses testing, one must ensure the same structure - all connections considered - for both the "before" and "after" presumed models. Based on this observation a new set of 11 models depicted in the Figure 5.3 was created.

Table 5.1: Coordinate sets of brain areas

	x	y	z
LS1a	-44	-42	60
LS1b	-32	-48	60
LS2	-46	-52	42
LSM1	-38	-30	58
RSM1	26	-36	64
SMA	4	-22	68

All the models featured equal number of areas for data measured before and after the therapy and contained just extrinsic input namely into LS1, LSM1, and SMA area - input representing right hand fingers movement and extrinsic input for coil position (there was not any modulatory input).

5.3.2 Areas

The next stage of DCM analysis was selection of substantial brain areas. Also in this case the clinical experience helps. But the other clue can be fMRI analysis result with significant active areas detection.
Here were selected five brain areas with significant activity related to the required task (finger movement), based on the second level analysis as provided by (SPM toolbox, 2012). In the case of LS1, stimulated directly by the rTMS coil, the question was however whether to apply the same second level analysis result for the coordinates estimation, or whether to define the coordinates explicitly as the coil target. In terms of medical experience it seems more logical to consider location of the coil as the stimulation area. The DCM results with this particular coordinate set also include more significant connections as well which proves this assumption. The Table 5.1 summarizes all coordinate sets and the Figure 5.4 shows the second level analysis result as a tool for their definition.

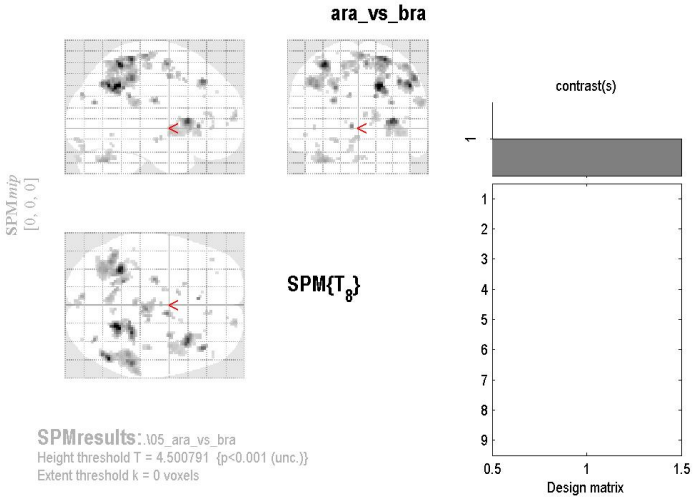

Statistics: ***p-values adjusted for search volume***

set-level		cluster-level			voxel-level					mm mm mm		
p	*c*	$p_{corrected}$	k_E	$p_{uncorrected}$	$p_{FWE-corr}$	$p_{FDR-corr}$	*T*	$(Z_=)$	$p_{uncorrected}$			
0.000	**61**	**0.000**	**305**	**0.000**	**0.392**	**0.094**	**10.86**	**4.58**	**0.000**	**20**	**-50**	**40**
					0.841	0.094	9.35	4.34	0.000	26	-36	64
					0.994	0.094	7.35	3.94	0.000	26	-50	34
		0.000	**284**	**0.000**	**0.591**	**0.094**	**10.29**	**4.50**	**0.000**	**-32**	**-48**	**60**
					0.999	0.094	6.90	3.84	0.000	-40	-56	40
					1.000	0.094	5.65	3.49	0.000	-34	-56	46
		0.000	**303**	**0.000**	**0.721**	**0.094**	**10.01**	**4.45**	**0.000**	**50**	**-58**	**40**
					0.977	0.094	7.92	4.07	0.000	54	-36	46
					1.000	0.094	6.43	3.72	0.000	46	-40	58
		0.000	**200**	**0.000**	**0.899**	**0.094**	**8.89**	**4.26**	**0.000**	**32**	**18**	**6**
					1.000	0.094	5.33	3.39	0.000	38	2	-4
					1.000	0.094	5.06	3.30	0.000	44	10	-4
		0.706	**26**	**0.040**	**0.982**	**0.094**	**7.80**	**4.05**	**0.000**	**40**	**32**	**44**
		0.226	**47**	**0.008**	**0.996**	**0.094**	**7.24**	**3.92**	**0.000**	**-22**	**-44**	**38**
					1.000	0.094	5.77	3.53	0.000	-20	-54	38
		0.706	**26**	**0.040**	**0.996**	**0.094**	**7.21**	**3.91**	**0.000**	**8**	**-2**	**60**
		1.000	**4**	**0.395**	**0.999**	**0.094**	**6.87**	**3.83**	**0.000**	**-6**	**28**	**2**
		0.082	**64**	**0.003**	**0.999**	**0.094**	**6.86**	**3.83**	**0.000**	**4**	**-22**	**68**
					1.000	0.094	5.37	3.40	0.000	-2	-16	68
		0.974	**14**	**0.118**	**0.999**	**0.094**	**6.80**	**3.81**	**0.000**	**-24**	**-14**	**26**

table shows 3 local maxima more than 8.0mm apart

Height threshold: T = 4.50, p = 0.001 (1.000) {p<0.001 (unc.)}
Extent threshold: k = 0 voxels, p = 1.000 (1.000)
Expected voxels per cluster, <k> = 5.950
Expected number of clusters, <c> = 30.96
Expected false discovery rate, <= 0.09

Degrees of freedom = [1.0, 8.0]
FWHM = 10.2 10.7 10.3 mm mm mm; 5.1 5.3 5.2 {voxels};
Volume: 1374936 = 171867 voxels = 1140.7 resels
Voxel size: 2.0 2.0 2.0 mm mm mm; (resel = 140.52 voxels)
Page 1

Figure 5.4: The second level analysis result - marked brain areas for whole group of patients - created in SPM toolbox

5.3.3 "Combinatorial explosion"

DCM analysis was created for 9 patients. It meant to get 198 models in total. This number is however only for data measured before rTMS therapy. The result set

doubles by DCM analysis for the data measured after rTMS therapy. The DCM analysis of one model is rather time-consuming and the computation for the whole set of models can easily take a few days. The problem could be solved much more effectively in principle by using some alternative dynamic system identification methods which would detect significant connections without the need to predefine models structure. Such methods are unfortunately not available now in the neuroimaging community. We try to summarize the first results of the approach in next chapter.

5.3.4 DCM drawbacks

DCM is undoubtedly an established and commonly used method for identification of functional brain organization from fMRI data. DCM processing however can have some drawbacks from the user's point of view. They are discussed here and based on our experience with fMRI data processing within writer's cramp study.
The predefinition of models is a complication not only for a user who does not have deep experience with fMRI, even educated experts have sometimes problems to establish the most appropriate model structure. As a result, a tedious trial-and-error loop must be performed to arrive at acceptable findings.
The DCM analysis of one model itself takes some time and the computation for a complete set of models can take a few days easily. Sometimes there is a specific additional uncertainty such as an alternative selection of a brain area coordinates which leads to additional structures to be considered. In the case of analysis of a therapy influence all these demands were doubled in principle (by data received after the therapy and their processing). These troubles could be considerably reduced if an alternative identification procedure were used in place of DCM that would automatically detect the internal structure of the most appropriate dynamical model.

5.4 Results

5.4.1 Individual assessment

The data set resulting from the medical experiment described in section 5.2 was restricted for practical reasons in terms of number of patients (9 in total). Consequently we will have some problems with statistical processing.
On the other hand, the DCM analysis results for particular patients can be qualitatively analyzed easily to reveal some basic rules appearing in all models for one particular patient, or appearing across the whole patient group for one particular model. In our case there was for instance the connection $LS1a \rightarrow LSM1$ included in majority of models. Interestingly, the strengths of this connection for a particular patient across the whole set of models were roughly equal. This observation can serve as a kind of "cross-check" when deducing about a particular connection significance.

5.4.2 Statistical processing: T test

The individual assessment results were to be statistically processed. Selected statistical tests were applied to connection strength (for particular connections and models, over all patients), comparing "before" and "after" numbers. The test was supposed to prove or disprove the hypothesis that the strength of a given connection in a given model had changed significantly.
The one-tailed paired T test was called for first. However, severe difficulties were issued, for two main reasons. First, there was the low number of patients in combination with measured data, corrupted by noise and other parasitic effects. Second, the normal distribution assumption of involved data was also questionable. Meaningful results were achieved only on high significance levels (say 20%). For typically used significance level 5% the hypothesis cannot be confirmed unfortunately. Two tables are related to this discussion. The Table 5.2 shows connection strength from LS1a area to RSM1 area for the whole patient group. The T test result executed on the one group of elements is in the Table 5.3. The fifth row determines one-tailed probability of t statistic and this value overreaches the significance level (5%).

Table 5.2: The strength of connection from LS1a to RSM1 across the whole patient group

LS1a - RSM1 - before	LS1a - RSM1 - after
-0.0164	-0.0350
-0.0026	0.2167
0.3951	0.0047
0.1519	0.0129
0.6320	0.6242
0.0642	-0.0539
0.0216	0.1821
0.2649	0.4547
0.2469	-0.0256

Table 5.3: T test result

	Set 1	Set 2
Mean	0.1953	0.1533
Variance	0.0464	0.0587
t stat	0.5831	
$P(T \leq t)$ (1)	0.2829	
t critical (1)	1.8595	

Table 5.4: Significant connections across the whole patient group - LS1 is location of the coil

connection	t statistic probability
LS1a-SMA - model 2	0.0381
LS1a-RSM1 - model 6	0.0109
LS1a-LS2 - model 6	0.0109
LS1a-SMA - model6	0.0858
RSM1-LS1a - model 6	0.0663
LS2-LS1a - model 6	0.0284

5.4.3 Statistical processing: Non-parametric statistical tests

The drawbacks of the parametric T-test discussed above can be eliminated by calling alternative non-parametric statistical tests. The Wilcoxon test and Sign test were applied, leading to similar conclusions. Only Wilcoxon test results are therefore discussed further.
The non-parametric tests show significant changes of six connections. The positive result is that five connections of those six are in the (reciprocal) model number 6, see section 5.4.4 for details. The non-parametric test results are summarized in Table 5.4. Four connections appear as significant (probability of t-statistic smaller than significance level 5% (three of them in model No. 6), two others are slightly above.

5.4.4 Results: Model 6

According to the nonparametric statistical test, the model number 6 features most significant changes in connection strengths over all involved patients. The model is given in the Figure 5.5. The model has only reciprocal connections. For almost all patients there is a remarkable reduction of strength of connections $LS1 \rightarrow RSM1$, $LS1 \rightarrow LS2$, $LS1 \rightarrow SMA$. This conclusion can be interpreted as a certain form of functional reorganization due to the rTMS therapy.

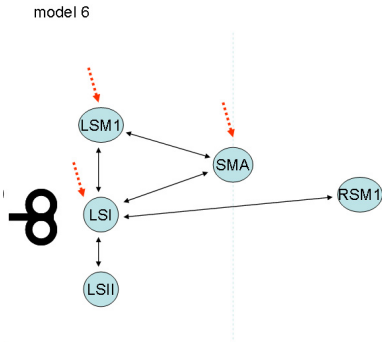

Figure 5.5: The model containing five significant connections

5.5 Conclusion

The chapter deals with DCM analysis of fMRI data measured on patients suffering from writer's cramp and subjected to an rTMS therapy. The main result is identification of a DCM model structure based on a non-parametric test performed on a reduced measured data set. Practical experience with DCM tools of the SPM toolbox is also discussed. The detailed description of the writer's cramp study from medical point of view and summary of all results (objective and subjective assessment) are given in (Havrankova, P. et al., 2010).

Chapter 6

System identification and fMRI data processing

6.1 Introduction

The main goal of this section is to define the complex dynamic system represented by brain areas within the context of the systems theory, and to cast it as a task for system identification. The system, as interpreted by the systems theory, is a complex object consisting of interconnected subsystems and components which transforms inputs into outputs and this transformation can be characterized by a mathematical model, usually in the form of differential equations. The input stimulus signals that enter into the brain system reflect the particular fMRI neurological experiment, and can be modeled as rectangular signals (on/off or active/inactive) as they correspond to hand motion, pictures projection, electrical stimulation etc. The measured outputs are BOLD signals which are usually visualized as volumetric 3D plots. They can also be viewed as rectangular for which at every time instance the measured value assumes a shape of a 3-dimensional array (cube). Hence the input-output behavior of the brain system can be measured experimentally. However the brain system is characterized by specific intrinsic structure comprised of two different parts called neurodynamics and hemodynamics, see Figure 6.1. The

input (stimulus) signals enter the faster dynamics (neurodynamics) representing the intrinsic interconnections among brain areas. Neurodynamics could be modeled by several first order systems, each corresponding to a given brain area and their intrinsic connections as is done by DCM in fact (Friston, K. J. et al., 2003). The neuronal response of every brain area is only observed in the fMRI data after passing through the slower hemodynamics part, which can be modeled as a simple system (filter) for each brain area separately. In contrast to the nonlinear balloon model used within DCM, higher order hemodynamic linear filters (at least order two) are necessary to capture the oscillatory behavior as shown in the next section concerning subspace identification methods used for fMRI data fitting.
So the task of brain behavior modeling can be formulated as a system identification problem. We can therefore apply classical black-box identification methods, commonly used in diverse industries for example in (Gannot, S. and Moonen, M., 2003), (Garnier, H. and Liuping, W., 2008), (Rice, J. K. and Verhaegen, M., 2008), (Yao, Y. and Gao, F., 2008), (Ljung, L., 1999), (Verhaegen, M. and Verdult, V., 2007), for fMRI data modeling and to observe if the fitting is sufficient. Further we can formulate more complex task of detection of intrinsic structure which can lead to a certain alternative to DCM.

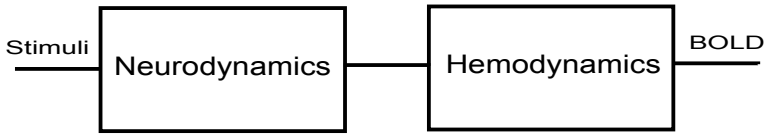

Figure 6.1: Brain dynamics system structure - two types of dynamics, at first faster dynamics, slower dynamics forms output BOLD signal in each activated brain area

This part reports on early attempts to approach the problem of modeling of the neural response of the human brain as a system identification and estimation task. The parametric identification method and simulated fMRI data are used for the hemodynamic response modeling. Our first steps are quite standard for control community: assuming linearity (and justifying it), finding a model of the response using some parametric identification techniques (ARX, OE, subspace methods...) and testing agreement between this model and the input output data for whole "cube of systems" - systems covering more brain areas.

The next step is modeling of MIMO (multiple input multiple output) systems including the intrinsic structure as DCM done that. Nowadays, inference about connectivity or coupling among brain areas, using fMRI, usually rests upon some form of Dynamic Causal Modeling (DCM). DCM uses Bayesian techniques to identify the underlying neuronal system in terms of coupling parameters. Crucially, one has to specify prior constraints on the sparsity or form of the connections and then test different models (forms) of connectivity. We work on a more efficient, direct approach. DCM is used to compare mathematical models with and without specific connections which entails fitting or inverting different models and then comparing their evidence. It is a methodology which enumerates possible models first, and then tests their validity using the conventional tools for testing statistic hypotheses (Friston, K. J. et al., 2003). The identification can take a considerable amount of time, especially when one compares large numbers of models. The main contribution of the part is to estimate the full connectivity of any DCM (under linear and first order assumptions) in a way that is extremely efficient. This may be especially useful in the context of DCM, because recent developments in model comparison allow one to evaluate the evidence of reduced models (in which some connections are omitted) given the estimates of a full model (Friston, K. J. et al., 2010).

6.2 MIMO identification - fMRI data fitting

This section summarizes first results of subspace identification experiments for fMRI simulated data. We focused on subspace N4SID identification methods implemented in System Identification Toolbox for Matlab (version 2007b). Subspace methods combine results of systems theory, geometry and numerical linear algebra (Katayama, T., 2005) (Faworeel, W. et al., 2000). They seem suitable for our task especially for their fine numerical reliability for MIMO system identification. In addition, they give rise to models in the state-space form directly. The simulated data sets differ in the signal-to-noise ratio factor (SNR) and in number of samples. Other parameters are the number of areas, interscan interval, and the number of conditions, see (SPM toolbox, 2012) for details. The data parameters are presented in the tables below for particular cases. Related tables

Table 6.1: The simulated data parameters - case 1,2

SNR	areas	TR	scans	cond.		
50	3	1.7	256	1		
onsets	20	45	113	154	203	240
duration	3	4	3	3	2	3

show the vector of onsets and vector of duration (definition of inputs, stimulation signal). The last piece of information for the SPM simulator is the matrix A defining the strength of connections, and the input matrix C. The results for particular parameters choices are the identified matrix A acquired from SPM toolbox by DCM estimation and then the (linear dynamic) model of simulated data acquired from the Identification Toolbox by help of subspace identification method (Identification toolbox, 2012).

6.2.1 Case 1

This example tests the quality of identification for simulated data with "good" parameters, see BOLD signals in Figure 6.2. The data set has enough samples and the signal-to-noise ratio is high, see Table 6.1. The input data is defined by vectors and the matrix of connection strength as well as the input matrix are also presented below in Equation 6.1.

$$A = \begin{pmatrix} -1 & 0 & 0 \\ 1 & -1 & 1 \\ 2 & 0 & -1 \end{pmatrix} \qquad C = \begin{pmatrix} 1 \\ 0 \\ 0 \end{pmatrix} \tag{6.1}$$

The DCM procedure gives fairly good results in terms of the identified matrix A which corresponds to the simulation model's A, see Equation 6.2 and 6.1 for comparison. The identification toolbox also proves useful here and fits successfully the simulated data by the identified linear model of order five, see Figure 6.3. We also bring the transfer function of model identified by subspace identification

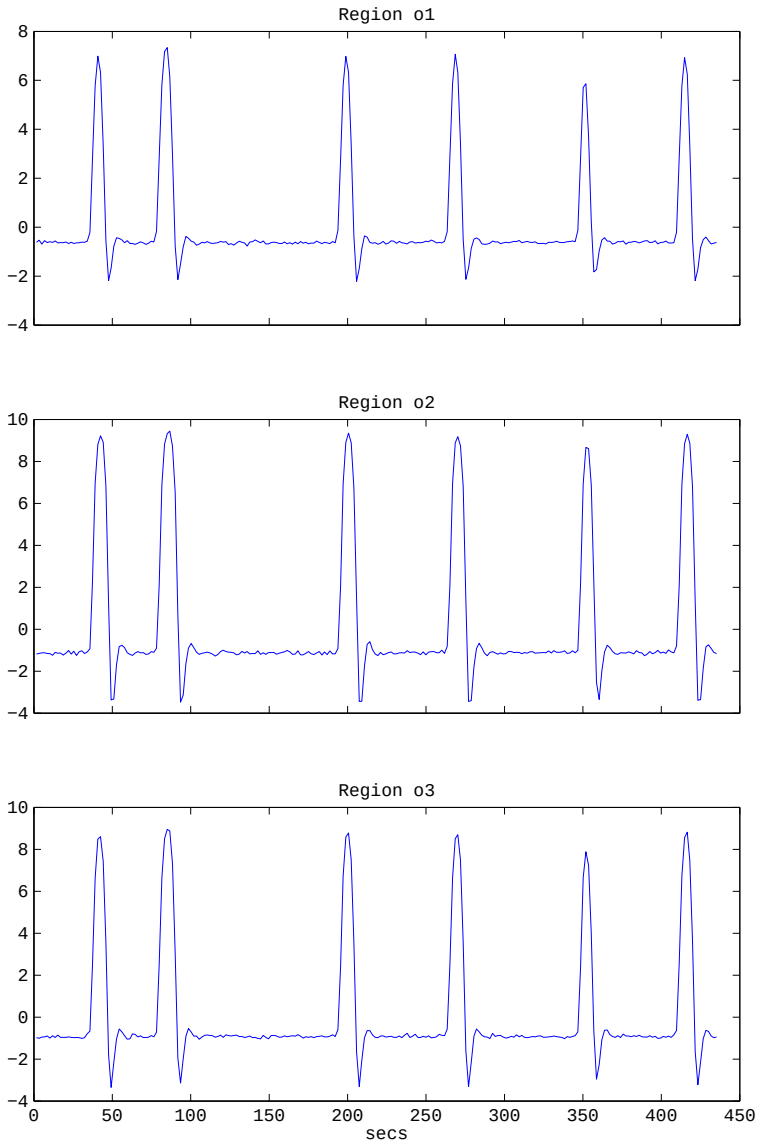

Figure 6.2: The simulated data for three areas - case 1 - created in SPM toolbox

method in zero-pole-gain format, see Equation 6.3.

$$A = \begin{pmatrix} -1 & 0 & 0 \\ 0.872 & -1 & 1.0716 \\ 1.9955 & 0 & -1 \end{pmatrix} \tag{6.2}$$

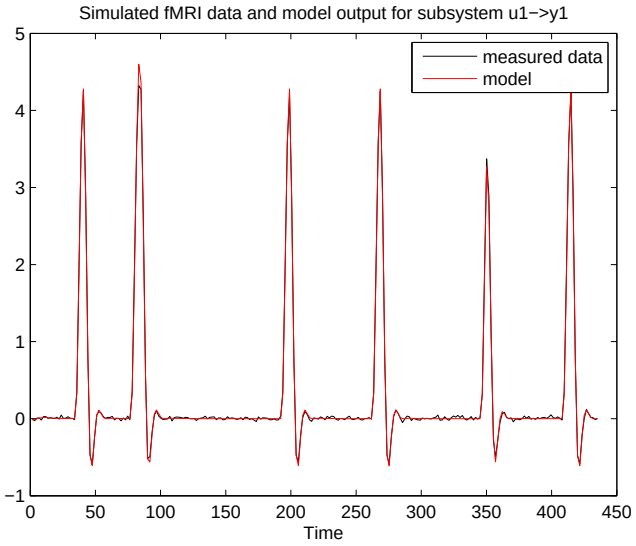

Figure 6.3: The simulated data and model for case 1

$$G_{u_1 y_1} = \frac{-0.52202(s - 1.631)(s + 0.1145)(s^2 + 0.6438s + 1.364)}{(s + 0.1115)(s^2 + 0.7257s + 0.3925)(s^2 + 0.8288s + 0.7242)} \tag{6.3}$$

6.2.2 Case 2

Simulated data with smaller signal-to-noise ratio equal to one are processed now. Other parameters remain unchanged from the previous case. To compare the noise effect for the cases 1 and 2 see Figures 6.2 and 6.4. The DCM procedure naturally embodies worse results than in the previous case which is shown in the matrix A again, see Equation 6.4. The system identification toolbox identifies the model with order three and the identified output series is confronted with simulated data in the Figure 6.5.

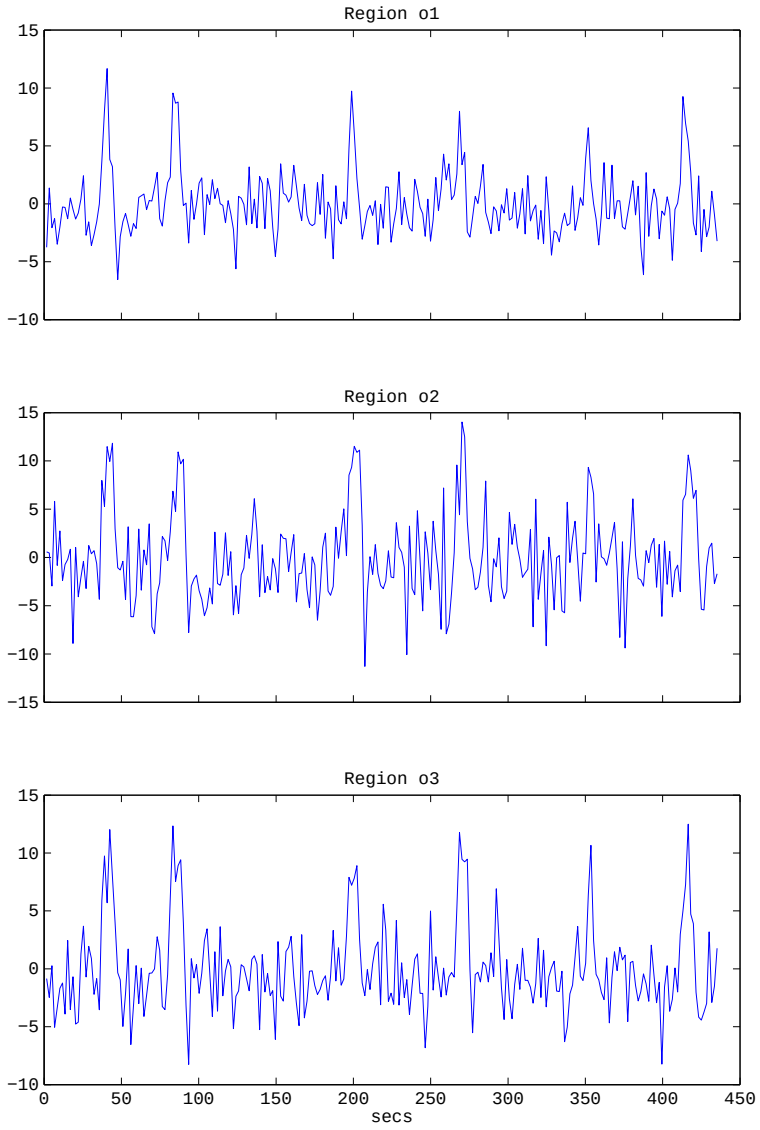

Figure 6.4: The simulated data for three areas - case 2 - created in SPM toolbox

$$A = \begin{pmatrix} -1 & 0 & 0 \\ 0.5057 & -1 & 0.5106 \\ 0.9121 & 0 & -1 \end{pmatrix} \tag{6.4}$$

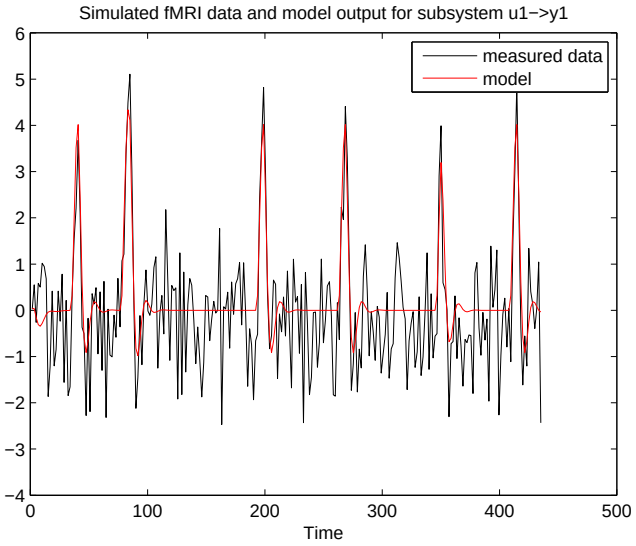

Figure 6.5: The simulated data and model for case 2

$$G_{u_1 y_1} = \frac{-0.54433(s - 1.527)(s + 0.1644)}{(s + 0.1663)(s^2 + 0.4181s + 0.2268)} \tag{6.5}$$

6.2.3 Case 3

A reduced 64-samples set was also generated by SPM simulator. The signal-to-noise ratio is the same as in the case 1 (= 50). The vectors of onsets and durations differ, see Table 6.2. The connectivity matrix is copied from the previous cases. DCM estimation result matrix A is below, see Equation 6.6.

$$A = \begin{pmatrix} -1 & 0 & 0 \\ 0.7566 & -1 & 1.1719 \\ 1.91 & 0 & -1 \end{pmatrix} \tag{6.6}$$

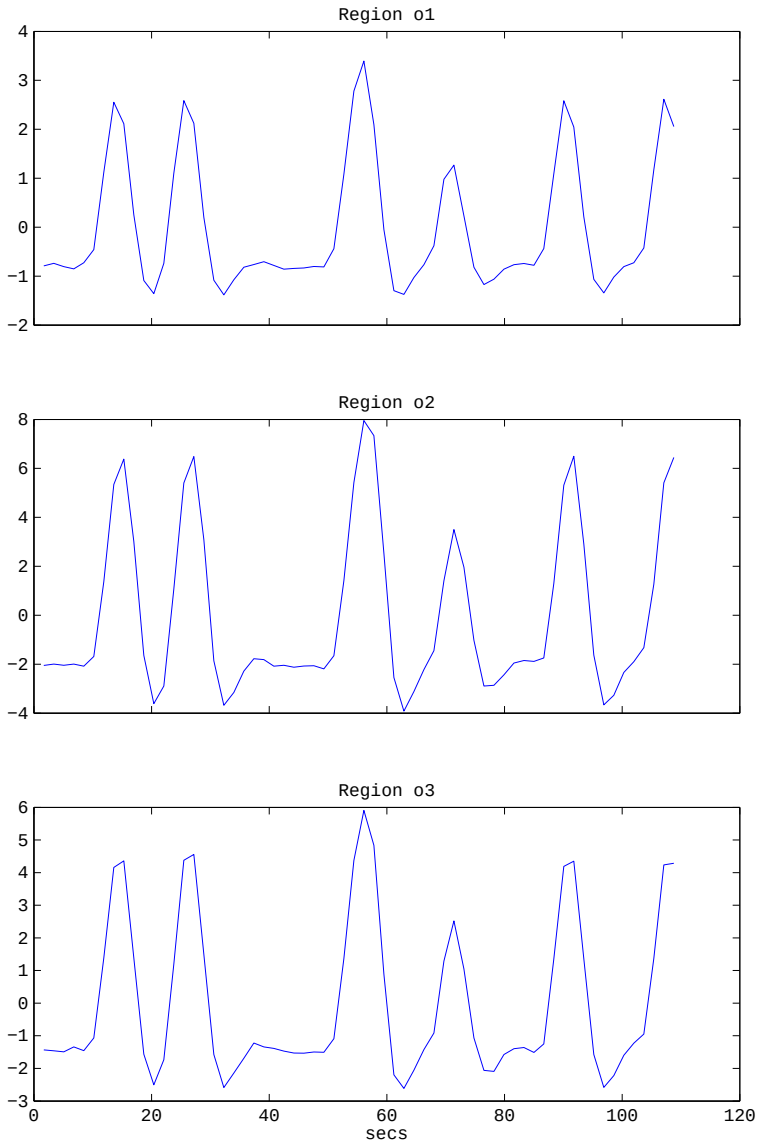

Figure 6.6: The simulated data for three areas - case 3 - created in SPM toolbox

Table 6.2: The simulated data parameters - case 3

SNR	areas	TR	scans	cond.		
50	3	1.7	64	1		
onsets	5	12	29	39	60	60
duration	2	2	3	1	2	2

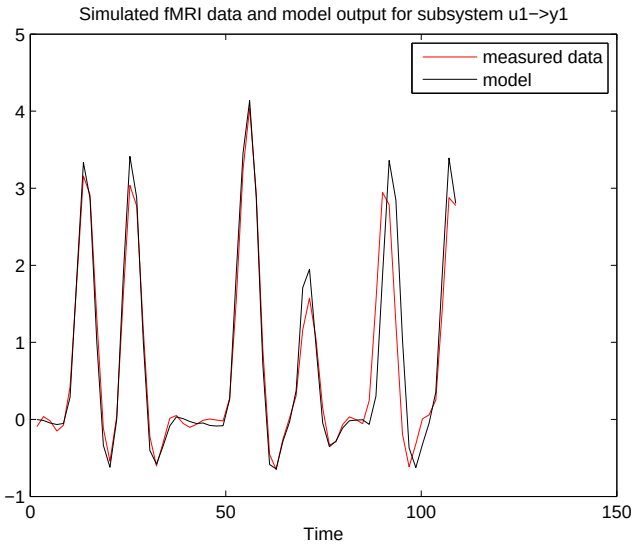

Figure 6.7: The simulated data and model for case 3

$$G_{u_1 y_1} = \frac{-0.048375(s - 4.673)(s + 0.1061)(s^2 + 1.506s + 2.401)}{(s + 0.1204)(s^2 + 0.77s + 0.244)(s^2 + 0.4313s + 0.5213)} \tag{6.7}$$

6.2.4 Case 4

Figures 6.8 and 6.9 show simulated fMRI data and their fitting by model. DCM result connectivity matrix and transfer function of model are

$$A = \begin{pmatrix} -1 & 0 & 0 \\ 0.7294 & -1 & 0.3973 \\ 0.6828 & 0 & -1 \end{pmatrix} \tag{6.8}$$

$$G_{u_1 y_1} = \frac{-1.192(s + 0.615)(s - 0.5842)}{(s + 0.82)(s^2 + 0.2743s + 0.2338)} \tag{6.9}$$

6.2.5 Conclusion

The simulation experiments carried out for various combinations of important parameters in the cases 1-4 prove applicability of subspace identification methods for fitting simulated fMRI data by linear dynamic higher-order models, without the necessity to pre-define the model structure. On basis of identified models we can say that every output hemodynamics filter should be modeled as at least a second order system with complex conjugate eigenvalues, reflecting the oscillatory response as shown in continuous transfer functions. At this moment it is not clear however how to interpret those dynamical models in terms of functional brain organization unfortunately, the DCM is certainly considerably farther in this regard. This issue will be therefore the direction of further research: how to interpret the linear identified model parameters in, say, a DCM-like manner.

6.3 Intrinsic structure detection

The next idea behind our approach is to estimate the significance of interconnections among the brain areas (so called intrinsic structure) by identifying the coupling among the states of an underlying linear state-space model. This is done by finding the state matrices describing the dynamics of neuronal states through the

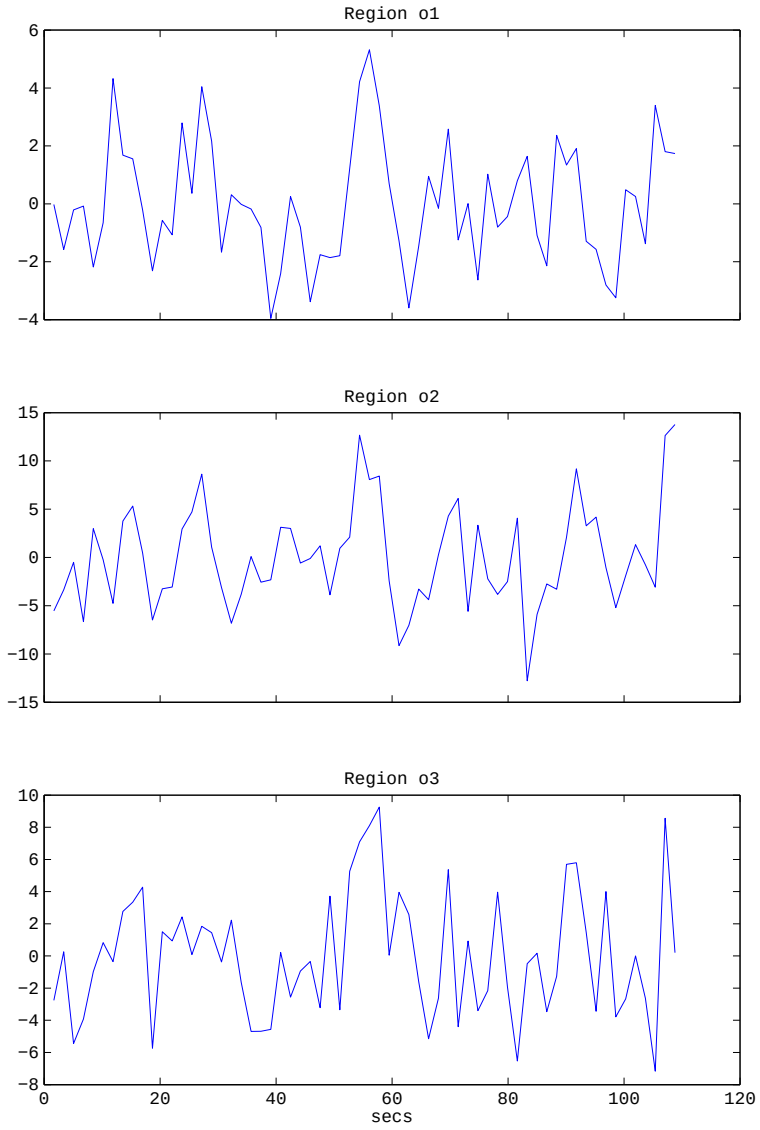

Figure 6.8: The simulated data for three areas - case 4 - created in SPM toolbox

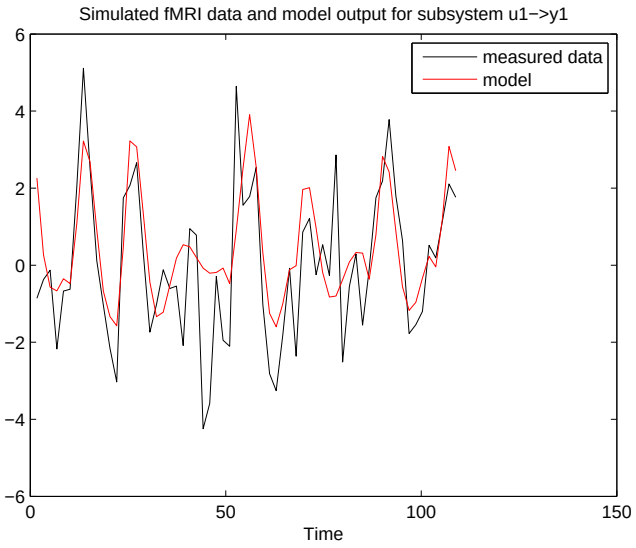

Figure 6.9: The simulated data and model for case 4

measured hemodynamic responses, using conventional linear system identification techniques, subspace identification methods here (N4SID especially). However, these methods do not apply constraints on the form of the state matrix. We finesse this problem by modeling the data with a number of hidden states that is greater than the number of observed brain areas. We then find a transformation of the hidden states that conforms to the known expected block structure of the state matrix appropriate for our problem. This transformation relies on the numerically reliable Schur decomposition of the original state matrix and related eigen decompositions. We can then interpret the transformed states in terms of neuronal and hemodynamic states. The transformed state matrix gives direct information on couplings between particular neuronal states, and also defines the mapping from neuronal to hemodynamic subsystems.

The subspace identification proves useful here and fits successfully the simulated data by the identified linear model as is shown in previous section; just for the last data set with smaller signal-to-noise ratio and number of samples the model is not able to fit data sufficiently. We can summarize that subspace identification methods are a promising technique for hemodynamic response fitting. So we attempt

to extend the identification procedure to the system including intrinsic structure detection.

6.3.1 Identification procedure for brain system structure

Subspace identification methods return a linear state space model in form Equation 6.10. The matrix A represents the dynamics, B is related to the inputs and C characterizes the outputs. The matrix D indicates direct connection from input to output in general. Choosing the linear model Equation 6.10 instead of the bilinear model used in DCM procedure (see chapter 4 for details) for brain area system description is intentional, ignoring so-called modulatory inputs motivated by simplicity. The hidden states x include certain transformation of all the neuronal and hemodynamic states in our model. This means the number of hidden states is much greater than the number of observations y (and that C is not a square matrix).

$$\begin{aligned} \dot{x}(t) &= \boldsymbol{A}x(t) + \boldsymbol{B}u(t) \\ y(t) &= \boldsymbol{C}x(t) + \boldsymbol{D}u(t) \end{aligned} \tag{6.10}$$

If we had the state space description in suitable form we could see intrinsic connections among selected brain areas directly. Unfortunately matrices A, B and C as a result of subspace methods are usually full and inappropriate to the specific structure of the brain system. Apparently it is necessary to transform the state space model into a realization reflecting separation of neurodynamics and hemodynamics. Matrix D of identified state space description is zero because there is no direct connection from input to output. One way to enforce this structure into the state space realization is a similarity transformation with a suitable transformation matrix T according to Equation 6.11.

$$
\begin{aligned}
A_{new} &= T^{-1}AT \\
B_{new} &= T^{-1}B \\
C_{new} &= CT \\
D_{new} &= D
\end{aligned}
\tag{6.11}
$$

These transformed matrices correspond to a transformation of variables in the form $x = Tx_{new}$, where x_{new} becomes our new desirable states that can be interpreted directly as neuronal and hemodynamic ones. The next section illustrates construction of the T matrix in a simple case which corresponds to the special brain structure according to Figure 6.10.

6.3.2 First order hemodynamics filter case

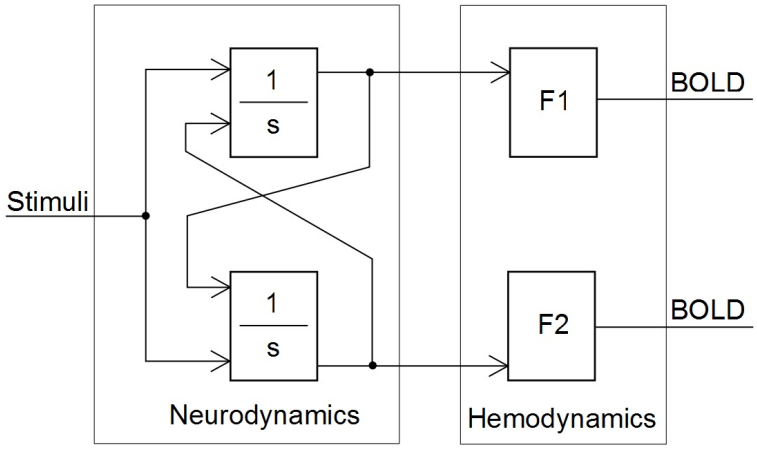

Figure 6.10: The detailed structure of brain system - neurodynamics is modeled by reciprocally connected first order systems. Each area has also own hemodynamics represented by higher order system

We consider a system including one input (stimulus) signal, two brain areas and two output (BOLD) signals, see Figure 6.10. The output filters for hemodynamics

modeling are considered as first order systems only for this moment (note that it does not fully correspond to orders necessary to model accurately hemodynamic filters as identified in the previous section 6.2., so it is not possible to use SPM toolbox as the data generator, and we use the generator according to system matrices Equation 6.13 instead). The subspace identification methods yield the full matrices A, B, and C, see Equation 6.12. The matrix D is zero (no direct throughputs are present in the system considered).

$$A = \begin{pmatrix} a_1 & a_2 & a_3 & a_4 \\ a_5 & a_6 & a_7 & a_8 \\ a_9 & a_{10} & a_{11} & a_{12} \\ a_{13} & a_{14} & a_{15} & a_{16} \end{pmatrix} \qquad B = \begin{pmatrix} b_1 \\ b_2 \\ b_3 \\ b_4 \end{pmatrix} \qquad C = \begin{pmatrix} c_1 & c_2 & c_3 & c_4 \\ c_5 & c_6 & c_7 & c_8 \end{pmatrix} \tag{6.12}$$

$$A = \begin{pmatrix} e_1 & 0 & g_1 & 0 \\ 0 & e_2 & 0 & g_2 \\ 0 & 0 & e_3 & c_{12} \\ 0 & 0 & c_{21} & e_4 \end{pmatrix} \qquad B = \begin{pmatrix} 0 \\ 0 \\ 1 \\ 1 \end{pmatrix} \qquad C = \begin{pmatrix} 1 & 0 & 0 & 0 \\ 0 & 1 & 0 & 0 \end{pmatrix} \tag{6.13}$$

However, the desired form is in Equation 6.13. This form reveals the specific structure of the brain system with the neuronal dynamics affected directly by the inputs and the hemodynamics projected immediately into the measured outputs. Matrix A contains the eigenvalues e_1, e_2 and the gain coefficients g_1, g_2 defining the hemodynamic SISO filters associated to a particular brain area. The lower right submatrix represents the (much faster) neurodynamics. The coefficients c_{12} and c_{21} are the crucial parameters which determine the intrinsic neuronal interconnections between the two modeled brain areas. The matrix B represents the structure of inputs and matrix C corresponds to the structure of outputs, in agreement with Figure 6.10.

Now we describe the sequence of similarity transformations steps leading from the full state-space model see Equation 6.12 to the structured form realization Equation 6.13 from which the coupling parameters c_{12} and c_{21} can be detected. We consider a system with one input and two brain areas, each modeled by first order dynamics and with corresponding two output BOLD signals. Each similarity

transformation follows the conventional rule in Equation 6.11. The first step is Schur decomposition applied to the identified dynamic matrix A. It yields zero elements under the main diagonal on which the eigenvalues are displayed. These are then ordered to separate the eigenvalues of hemodynamics (slow) and neurodynamics (fast). The subsequent steps are devised to impact the remaining parts of state space description and to preserve the effect of the previous transformation steps. In this way, the eigenvectors of a selected submatrix of the new dynamic matrix A are calculated and used for diagonalization of the submatrix representing hemodynamics filters, and the null space of output matrix C is used for zeroing its selected elements. We also use inverse submatrix for adjustment of parts concerning gain coefficients of output (hemodynamic) filters. All steps are detailed in a Matlab pseudocode-form see Figure 6.11, and are illustrated by a numerical example in the case study in the next section.

```
>>[T1,A1] = schur(A)
>>[T2,A2] = ordschur(T1,A1,[1,2,3,4])
>>G2 = ss(T2\A*T2, T2\B, C*T2, 0);

>>[t1,aj1] = eig(G2.a(1:2,1:2));
>>C2 = G2.c*blkdiag(t1,eye(2));
>>T3 = T2*blkdiag(t1,eye(2))*[eye(4,2), null(C2)];
>>G3 = ss(T3\G2.a*T3, T3\G2.b, G2.c*T3, 0);

>>t2 = inv(G3.a(1:2,3:4));
>>T4 = [eye(2) zeros(2);zeros(2) t2];
>>G4 = ss(T4\G3.a*T4, T4\G3.b, G3.c*T4, 0);}
```

Figure 6.11: Matlab pseudo-code for similarity transformation

Note that the transformation matrix $T1$ resulting from the Schur decomposition is applied to identified dynamic matrix A and the Matlab function *ordschur.m* is able to sort eigenvalues on the main diagonal, so we obtain new state space description $G2$ with dynamic matrix $G2.a$ containing separated hemodynamic and neurodynamic eigenvalues. The next transformation with the matrix $T3$ includes null space of output matrix $C2$, and the eigenvectors of the hemodynamic part

of matrix $G2.a$ are used as well. The hemodynamic part of the dynamic matrix $G2.a$ is now diagonal due to appropriate eigenvectors application, the input matrix $G2.b$ is also modified (zeroing of values representing input to the hemodynamic filters). The transformation also ensures zeroing of values representing output from neurodynamic part in the matrix $G2.c$. We can see that there is no external input into the hemodynamic filters, only from the neurodynamic part, and there is no measured output from the neurodynamic part, which is desirable. The last important transformation step is $G3.a$ adjustment, and we namely want to impact the submatrix related to the hemodynamic filters. So we apply transformation matrix $T4$ including inverse of a submatrix of $G3.a$ to diagonalize appropriate submatrix. So the almost final result of these transformation steps is the dynamic matrix $G4.a$ with eigenvalues and gains of hemodynamic filters in the upper part, and the submatrix concerning neurodynamics at the bottom which contains interconnections between two areas on the next diagonal. Matrices $G4.b$ and $G4.c$ are also modified according to the form in Equation 6.13 and they reflect brain system structure (no external input into hemodynamic filters, no external output from the neurodynamic part).

6.3.3 Case study

Data for the identification procedure were generated using the system Equation 6.14 with structure according to Figure 6.10.

$$A = \begin{pmatrix} -1 & 0 & 1 & 0 \\ 0 & -2 & 0 & 2 \\ 0 & 0 & -10 & 0 \\ 0 & 0 & 5 & -10 \end{pmatrix} \qquad B = \begin{pmatrix} 0 \\ 0 \\ 1 \\ 1 \end{pmatrix} \qquad C = \begin{pmatrix} 1 & 0 & 0 & 0 \\ 0 & 1 & 0 & 0 \end{pmatrix} \tag{6.14}$$

Matrices in Equation 6.15 illustrate the state space description of a system with two areas modeled by first order systems, one input and two outputs, as identified by a subspace identification method (Faworeel, W. et al., 1999)(Faworeel, W. et al., 2000)(Katayama, T., 2005) implemented in the functions of System Identification Toolbox for Matlab (Identification toolbox, 2012).

$$A = \begin{pmatrix} -2.36 & 12.22 & -7.52 & -11.40 \\ -4.91 & -5.06 & 7.07 & 4.15 \\ 3.14 & -0.13 & -2.18 & -3.02 \\ -0.09 & 12.61 & -8.61 & -13.39 \end{pmatrix} \qquad B = \begin{pmatrix} 3.15 \\ -1.22 \\ 0.38 \\ 3.44 \end{pmatrix} \tag{6.15}$$

$$C = \begin{pmatrix} -1.16 & 0.20 & -0.27 & 1.16 \\ -1.79 & 0.50 & 0.14 & 1.80 \end{pmatrix}$$

$$A = \begin{pmatrix} -0.999 & 0 & 0.999 & 0 \\ 0 & -2.001 & 0 & 2.001 \\ 0 & 0 & -10.071 & -0.021 \\ 0 & 0 & 4.988 & -9.986 \end{pmatrix} \qquad B = \begin{pmatrix} 0 \\ 0 \\ 1.001 \\ 0.999 \end{pmatrix} \tag{6.16}$$

$$C = \begin{pmatrix} 1 & 0 & 0 & 0 \\ 0 & 1 & 0 & 0 \end{pmatrix}$$

Particular similarity transformation steps described in 6.3.2 leading to state space description in Equation 6.13 were applied. The final result reflecting the desired structure is in Equation 6.16. We can also see in Figure 6.12 that step response of transformed system is the very same as step response of the data generator. Therefore we did not change the input-output response of the originally identified system by similarity transformation and we found one of the equivalent state realization that reveal coupling structure between neurodynamics and hemodynamics. Here the $(4, 3)$ element of the matrix indicates the connection between the two areas, that would be visualized in the DCM diagrams style as in Figure 6.13.

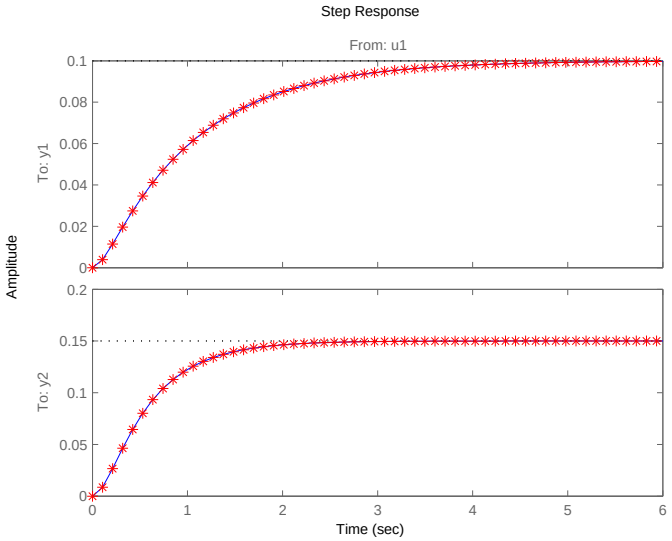

Figure 6.12: Step response of identified transformed system and original system for the data generation are the same

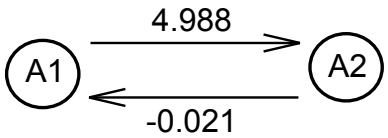

Figure 6.13: Diagram of the final detected connections

Chapter 7

Conclusion

The system identification methods for fMRI data processing were presented in this thesis. First we completed a comprehensive overview of fMRI area from systems identification viewpoint, it is possible to find it in State-of-the-art and chapter 3. We also discussed SPM toolbox using from user's point of view within Writer's cramp study - presented in chapter 5.
In this thesis we proposed to formulate the task of detection of brain areas structure within the well-established and mature framework of system identification as a promising alternative to Dynamic Causal Modeling which is based on statistical hypothesis-testing. The motivation for developing this alternative approach comes from the need to reduce the computational burden so that the fMRI data can be processed in real-time. We proposed a concrete computational procedure based on the popular subspace identification techniques applied to the measured (simulated respectively) fMRI data combined with a similarity transformation which enforces the structure into the problem (this structure accounts for the separation of dynamics into the neuronal and hemodynamic part). The procedure was demonstrated by a simple simulation example in chapter 6.

7.1 Main results

The goals of the thesis as prescribed in Chapter 2 were fulfilled in the following manner.

- "Goal 1" is fully addressed in the thesis. We provide a comprehensive review of techniques and procedures commonly used in fMRI area especially from systems identification point of view. We present elementary terminology of fMRI area, basic principle of fMRI measurement and we also mention some basic methods of fMRI data modeling, see State-of-the-art, chapters 3 and 4.

- "Goal 2" has been fulfilled as well. We present commonly used tool for fMRI processing called SPM toolbox in chapter 4. We also give a description of Dynamic Causal Modeling technique for intrinsic structure detection and discuss some advantages and drawbacks of that from user's viewpoint within cooperation with Department of Neurology, 1^{st} Faculty of Medicine, Charles University in Prague and project called Writer's cramp study. We develop joint paper "Repetitive TMS of the somatosensory cortex improves writer's cramp and enhances cortical activity" published in Neuro Endocrinology Letters (IF 1.621). The results and our experience with DCM implemented in SPM toolbox are shown in chapter 5.

- Finally, "Goal 3" as prescribed in chapter 2, has been developed in the thesis too. We present subspace identification methods for fMRI data modeling and consider them as certain alternative to DCM procedure, see chapter 6. We show intrinsic structure detection on simplified case - paper "Dynamic causal modeling and subspace identification methods" is published in Biomedical Signal Processing (IF 1.000).

7.2 Suggestions for Future Research

The thesis raises some questions and problems that have not been answered yet.

7.2.1 Intrinsic structure detection

Surely the proposed and demonstrated method simplifies the problem a lot by the assumption of a linear model: the bilinear terms in the neuronal dynamics considered within the DCM framework are neglected here because modification of subspace identification techniques for bilinear models does not appear to be straightforward and is subject to further research.
The model of hemodynamics is also considered as an LTI model although currently some nonlinear models (such as the Balloon model) are used within the fMRI community. In addition, the procedure is fully functional for first order hemodynamic filters only. It was observed though that when using system identification techniques to some fMRI data generated by the SPM toolbox, every output hemodynamics filter should be modeled as at least a second order system with complex conjugate eigenvalues, reflecting the oscillatory response as shown in section 6.2. The similarity transformations then become more complicated and the procedure proposed in this thesis cannot handle it at this moment

7.2.2 ARX and OE models

One way to intrinsic structure detection could be also using other parametric identification methods, ARX or OE models. Our idea is to identify model with suitable order corresponding to number of brain areas and with adequate order of output filters for hemodynamic response shaping. Then we would look for solution of nonlinear equation system with joint neurodynamics parameters, see Figure 7.1.

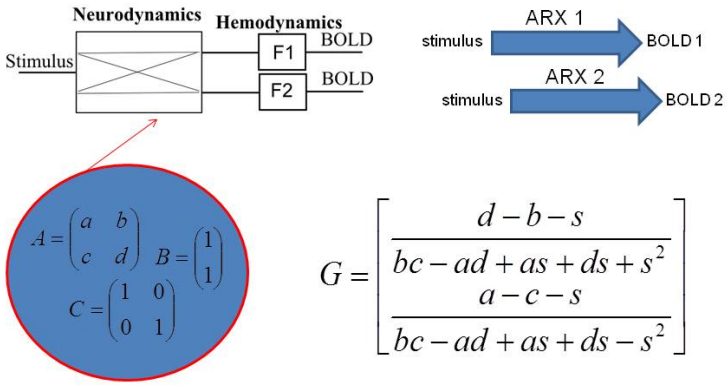

Figure 7.1: Other parametric methods using

Bibliography

Antsaklis, P. J. and Michel, A. N. (1997), *Linear Systems*, Birkhäuser, Boston.

Bailey, D. L., Townsend, D. W., Valk, P. E. and Maisey, M. N. (2005), *Positron Emission Tomography: Basic Sciences*, Springer-Verlag.

Belliveau, J. W. and col. (1991), 'Functional mapping of the human visual cortex by magnetic resonance imaging', *Science* **254** , 716–719.

Boynton, G., Engel, S., Glover, G. and Heeger, D. (1996), 'Linear systems analysis of functional magnetic resonance imaging in human V1', *Journal of Neuroscience* **16** , 4207–4221.

Buxton, R. B. and Frank, L. R. (1997), 'A model for the coupling between cerebral blood flow and oxygen metabolism during neural stimulation', *Journal of Cerebral Blood Flow and Metabolism* **17** , 64–72.

Buxton, R. B., Wong, E. C. and Frank, L. R. (1998), 'Dynamics of Blood Flow and Oxygenation Changes During Brain Activation: The Balloon Model', *Magnetic Resonance in Medicine* **39** , 855–864.

Calhoun, V. D., Adali, T., Hansen, L. K., Larsen, J. and Pekar, J. J. (2003), ICA of functional MRI data: an overview, *in* '4th International Symposium on Independent Component Analysis and Blind Signal Separation', Nara, Japan.

Cohen, D. and Halgren, E. (2004), *Magnetoencephalography, Encyclopedia of Neuroscience*, Elsevier.

Ethofer, T., Anders, S., Erb, M., Herbert, C., Wiethoff, S., Kissler, J., Grodd, W. and Wildgruber, D. (2005), 'Cerebral pathways in processing of affective prosody: A dynamic causal modeling study', *NeuroImage* **30** , 580–587.

Faworeel, W., Moor, B. D. and Overschee, P. V. (1999), 'Subspace identification of bilinear systems subject to white inputs', *IEEE Transactions on Automatic Control* **44** , 1156–1165.

Faworeel, W., Moor, B. D. and Overschee, P. V. (2000), 'Subspace state space system identification for industrial processes', *Journal of Process Control* **10** , 149–155.

Friston, K. J. (2002), 'Bayesian Estimation of Dynamical Systems: An Application to fMRI', *NeuroImage* **16** , 513–530.

Friston, K. J., Ashburner, J., Frith, C. D., Poline, J. B., Heather, J. D. and Frackowiak, R. S. J. (1995), 'Spatial registration and normalization of images', *Human Brain Mapping* **2** , 165–189.

Friston, K. J., Ashburner, J., Kiebel, S. J., Nichols, T. E. and Penny, W. D. (2007), *Statistical Parametric Mapping: The Analysis of Functional Brain Images*, Academic Press.

Friston, K. J., Buechel, C., Fink, G. R., Morris, J., Rolls, E. and Dolan, R. J. (1997), 'Psychophysiological and Modulatory Interactions in Neuroimaging', *NeuroImage* **6** , 218–229.

Friston, K. J., Frith, C. D., Liddle, P. F. and Frackowiak, R. S. J. (1991), 'Comparing functional (PET) images: the assessment of significant change', *Journal of Cerebral Blood Flow and Metabolism* **11** , 690–699.

Friston, K. J., Harrison, L. and Penny, W. (2003), 'Dynamic Casual Modeling', *NeuroImage* **19** , 1273–1302.

Friston, K. J., Holmes, A. P., Worsley, K. J., Poline, J. B., Frith, C. D. and Frackowiak, R. S. J. (1995), 'Statistical parametric maps in functional imaging: A general linear approach', *Human Brain Mapping* **2** , 189–210.

Friston, K. J., Jezzard, P. J. and Turner, R. (1994), 'Analysis of functional MRI time-series', *Human Brain Mapping* **1** , 153–171.

Friston, K. J., Li, B. and Stephan, K. E. (2010), 'Network discovery with DCM', *NeuroImage* **56** , 1202–1221.

Friston, K. J., Mechelli, A., Turner, R. and Price, C. J. (2000), 'Nonlinear Responses in fMRI: The Balloon Model, Volterra Kernels, and Other Hemodynamics', *NeuroImage* **12** , 466–477.

Friston, K. J., Penny, W., Phillips, C., Kiebel, S., Hinton, G. and Ashburner, J. (2002), 'Classical and Bayesian Inference in Neuroimaging: Theory', *NeuroImage* **16** , 465–483.

Gannot, S. and Moonen, M. (2003), 'Subspace methods for multimicrophone speech dereverberation', *Journal of Applied Signal Processing* **11** , 1074–1090.

Garnier, H. and Liuping, W. (2008), *Identification of continuous-time models from sampled data*, Springer, London.

Geuns, R. J., Wielopolski, P. A., Bruin, H. G., Rensing, B. J., Ooijen, P. M. A., Hulshoff, M., Oudkerk, M., Feyter, P. J. and Rensing, B. J. (1999), 'Basic principles of magnetic resonance imaging', *Progress in Cardiovascular Diseases* **42** , 149–156.

Harrison, L. M., Penny, W. and Friston, K. J. (2003), 'Multivariate autoregressive modeling of fMRI time series', *NeuroImage* **19** , 1477–1491.

Havrankova, P., Jech, R., Walker, ND., Operto, G., Tauchmanova, J., Vymazal, J., Dusek, P., Hromcik, M. and Ruzicka, E. (2010), 'Repetitive TMS of the somatosensory cortex improves writer's cramp and enhances cortical activity', *Neuro Endocrinology Letters* **31** , 73–86.

Hämäläinen, M., Hari, R., Ilmoniemi, R., Knuutila, J. and Lounasmaa, O. V. (1993), 'Magnetoencephalography – theory, instrumentation, and applications to noninvasive studies of signal processing in the human brain', *Reviews of Modern Physics* **65** , 413–497.

Holmes, A. and Friston, K. (1998), 'Generalisability, random-effects and population inference', *NeuroImage* **7** , S754.

Hornak, J. P. (2008), *The basics of MRI*, Interactive learning Software.

Jech, R., Havrankova, P., Walker, N., Tauchmanova, J. and Vymazal, J. (2008), fMRI in patients with writer's cramp treated by (rTMS) of the primary somatosensory cortex, *in* '14th Annual meeting of the Organization for Human Brain Mapping', Melbourne, Australia.

Katayama, T. (2005), *Subspace methods for system identification*, Springer, London.

Kiebel, S. J., David, O. and Friston, K. J. (2006), 'Dynamic casual modeling of evoked responses in EEG/MEG with lead field parametrization', *NeuroImage* **30** , 1273–1284.

Ljung, L. (1999), *System Identification - Theory For the User*, Prentice Hall.

Miyapuram, K. P. (2008), Introduction to fMRI: experimental design and data analysis, PhD thesis, University of Cambridge.

Ogawa, S., Lee, T., Kay, A. and Tank, D. (1990), 'Brain magnetic resonance imaging with contrast dependent on blood oxygenation', *Proc. Natl. Acad. Sci. U.S.A.* **87** , 9868–9872.

Overschee, P. V. and Moor, B. D. (1996), *Subspace identification for linear systems - Theory, Implementation, Applications*, Kluwer academic publisher, London.

Penny, W. D., Stephan, K. E., Mechelli, A. and Friston, K. J. (2004), 'Comparing dynamic casual models', *NeuroImage* **22** , 1157–1172.

Rice, J. K. and Verhaegen, M. (2008), Distributed Control: A sequentially semi-separable approach, *in* '47th IEEE Conference on Decision and Control', Mexico.

Roebroeck, A., Formisano, E. and Goebel, R. (2005), 'Mapping directed influence over the brain using Granger causality and fMRI', *NeuroImage* **25** , 230–242.

Smith, S. M. (2004), 'Overview of fMRI analysis', *The British Journal of Radiology* **77** , 167–175.

Stephan, K. E., Harrison, L., Penny, W. and Friston, K. J. (2004), 'Biophysical models of fMRI responses', *Current Opinion in Neurobiology* **14** , 629–635.

Verhaegen, M. and Verdult, V. (2007), *Filtering and System Identification: A Least Squares Approach*, Cambridge University Press.

Yao, Y. and Gao, F. (2008), 'Subspace identification for two-dimensional dynamic batch process statistical monitoring', *Chemical Engineering Science* **63** , 3411–3418.

Zhenghui, H., Xiaohu, Z., Huafeng, L. and Pengcheng, S. (2009), 'Nonlinear Analysis of the BOLD Signal', *EURASIP Journal on Advances in Signal Processing* .

Faculty of Medicine, Masaryk University Brno (2012), 'Faculty of Medicine, Masaryk University Brno', *fmri.mchmi.com/main_index.php*.

Identification toolbox, The Mathworks (2012), 'Identification Toolbox for Matlab', *http://www.mathworks.com*.

The Department of Mathematics and Statistics, McGill University and Statistics, McGill University, Q. (2012), 'The Department of Mathematics and Statistics', *http://www.math.mcgill.ca/*.

Radiopaedia.org (2012), 'Radiopaedia', *http://radiopaedia.org/*.

SPM toolbox (2012), 'University College London, Institute of Neurology', *www.fil.ion.ucl.ac.uk/spm*.

SPM toolbox manual, Department of Imaging Neuroscience (2012), 'University College London, Institute of Neurology', *www.fil.ion.ucl.ac.uk/spm/doc/manual.pdf*.

List of Author's Publications

Publications of the author related directly to the thesis

Journal Papers

[1] Tauchmanová J.; Computer controlled switching device for deep brain stimulation, *Acta Polytechnica*, 2007, vol. 47, p.4-5.(100%)

[2] Nováková J., Hromčík M. and Jech R.; Dynamic Causal Modeling and subspace identification methods, *Biomedical Signal Processing and Control*, 2012, vol.7, p. 365-370. ISSN 1746-8094. (Impact factor 2012 is 1.000). (45%)

[3] Havránková P., Jech R., Walker ND., Operto G., Tauchmanová J., Vymazal J., Dušek P., Hromčík M. and Růžička E.; Repetitive TMS of the somatosensory cortex improves writer's cramp and enhances cortical activity, *Neuro Endocrinology Letters*, 2010, vol.31, p. 73-86. (Impact factor 2010 is 1.621).(10%)

[4] Hoskovcová M., Ulmanová O., Šprdlík O., Sieger T., Nováková J., Jech R. and Růžička E.; Disorders of Balance and Gait in Essential Tremor Are Associated with Midline Tremor and Age, *The Cerebellum*, In Press, ISSN 1473-4230. (Impact factor 2011 is 3.207).(12%)

Conference Papers

[5] Tauchmanová J. and Hurák Z.; Localization of hemodynamic response from fMRI data using system identification and estimation techniques; *Proceedings of 16th Interantional Conference of Process Control 2007 [CD-ROM].* Bratislava: Slovenská technická univerzita, 2007. ISBN 978-80-227-2677-1.

[6] Tauchmanová J. and Jech R. and Havránková and Hromčík M.; Subspace identification methods and fMRI analysis; *Proceedings of the IEEE Engineering in Medicine and Biology Society, 2008 [CD-ROM].* Vancouver. ISBN 978-1-4244-1814-5.

[7] Tauchmanová J. and Hromčík M. and Jech R.; SPM Matlab Toolbox; *Proceedings of the Technical Computing Prague, 2008 [CD-ROM].* Prague. ISBN 978-80-7080-692-0.

[8] Jech R., Havránková, Walker N., Tauchmanová J., Vymazal J. and Růžička E.; fMRI in patients with writer's cramp treated by repetitive transcranial magnetic stimulation (rTMS) of the primary somatosensory cortex; *OHBN 2008 Abstracts on CD [CD-ROM].* Minneapolis, 2008.

[9] Tauchmanová J. and Hromčík, M.; The first results of systems identification methods for fMRI data; *17th International Conference on Process Control´09 [CD-ROM].* Bratislava, 2009. ISBN 978-80-227-3081-5.

Unpublished lecture

[10] Tauchmanová J. and Hromčík, M.; System identification methods for biomedical data processing; *Research colloquium in TU Delft.* Delft, 2010.

Vita

Jana Nováková was born on July 27, 1983 in Jilemnice, Czech Republic. She got her Ing. degree (Czech equivalent to MSc.) in Technical Cybernetics, with major in control systems, at the Faculty of Electrical Engineering, Czech Technical University in Prague (FEE CTU), Czech Republic, in 2007. After graduation she got a position of a full time researcher at the Department of Control Engineering at FEE CTU.

Jana Nováková was also involved in a project of Department of Neurology, 1^{st} Faculty of Medicine, Charles University in Prague focused on a neurological diseases studies. Teaching activities at FEE CTU cover exercises and labs of the Systems and Models, Systems and Control. She supervised two bachelor thesis.

Jana Nováková kept contact with leading universities and research institutes abroad. He has made a visit to TU Delft (professor Michel Verhaegen) for participation in research colloquium.

Jana Nováková presents her results regularly at some international conferences.

Address:

Department of Control Engineering,
Faculty of Electrical Engineering,
Czech Technical University in Prague
Karlovo náměstí 13/E,
121 35, Prague 2
Phone: +420 2 2435 7681
E-mail: tauchjan@fel.cvut.cz

This thesis was typeset with LaTeX 2$_\varepsilon$[1] by author.

[1] LaTeX 2$_\varepsilon$ is an extension of LaTeXwhich is a collection of macros for TeX. TeX is a trademark of the American Mathematical Society.